Title: Quantum circuits on neutral atom computers

Speakers: Mark Saffman

Collection: Cold Atom Molecule Interactions (CATMIN)

Date: July 15, 2022 - 10:50 AM

URL: https://pirsa.org/22070014

Abstract: "Neutral atom quantum computers with Rydberg mediated entangling gates are rapidly advancing as a leading platform for quantum information processing. I will present recent results running quantum algorithms for preparation of multi-qubit GHZ states, phase estimation, and hybrid quantum/classical optimization. Future fault tolerant quantum processors will require large numbers of qubits, high fidelity gates, and error correcting protocols. Work in progress towards fault tolerance including preparation of arrays of more than 1000 atoms, mid-circuit measurements, and multi-qubit gates will be presented"

Quantum circuits on neutral atom computers

M. Saffman

WISCONSIN QUANTUM INSTITUTE
Quantum Science and Engineering at UW–Madison

wqi.wisc.edu

WISCONSIN
UNIVERSITY OF WISCONSIN–MADISON

ColdQuanta

HQAN

Q-NEXT
NEXT GENERATION QUANTUM SCIENCE AND ENGINEERING

NSF

WARF
Wisconsin Alumni Research Foundation

U.S. DEPARTMENT OF ENERGY

Collective coupling of atoms and light

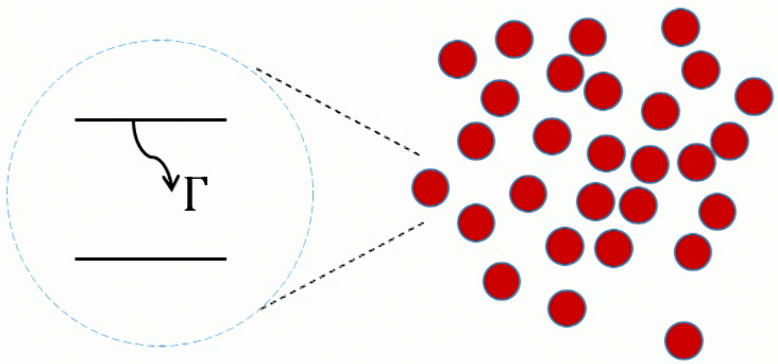

Super-radiance

Sub-radiance

Directed emission

2

2

Collective coupling of atoms and light

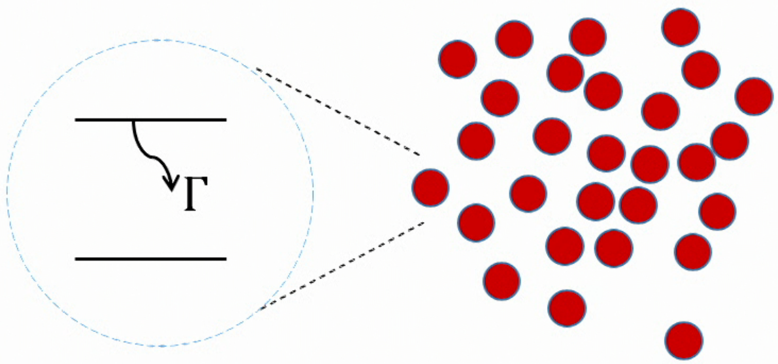

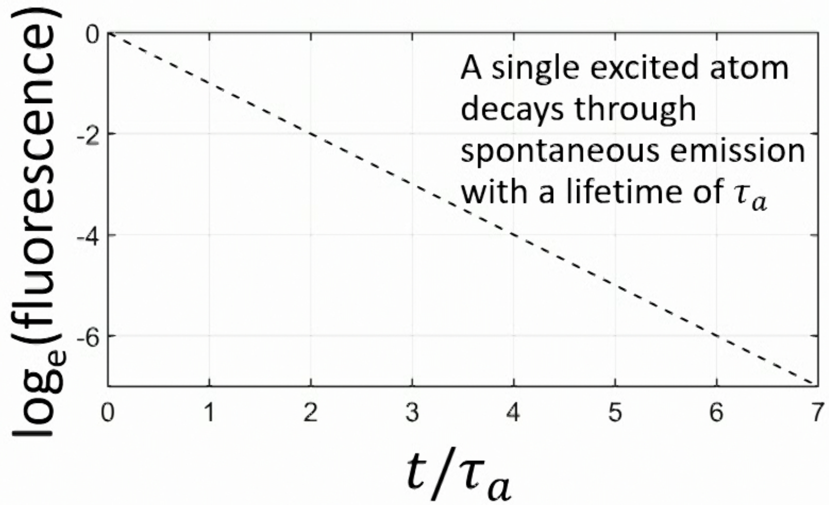

Super-radiance

Sub-radiance

Directed emission

2

2

A disordered ensemble of emitters

- An ensemble of atoms can decay superradiantly ($\tau < \tau_a$) or subradiantly ($\tau > \tau_a$) (Dicke, 1954)

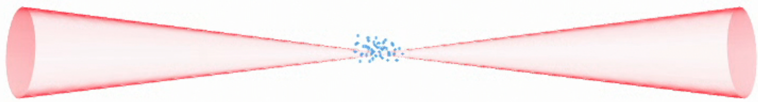

PRX QUANTUM **3,** 010338 (2022)

Spatial Coherence of Light in Collective Spontaneous Emission

D. C. Gold, P. Huft, C. Young, A. Safari, T. G. Walker, M. Saffman, and D. D. Yavuz*

A disordered ensemble of emitters

- An ensemble of atoms can decay superradiantly ($\tau < \tau_a$) or subradiantly ($\tau > \tau_a$) (Dicke, 1954)

- In a disordered sample in-phase super-radiant modes decay faster, leaving anti-phased sub-radiant modes that are spatially correlated

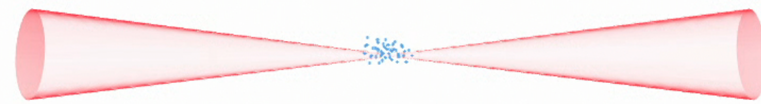

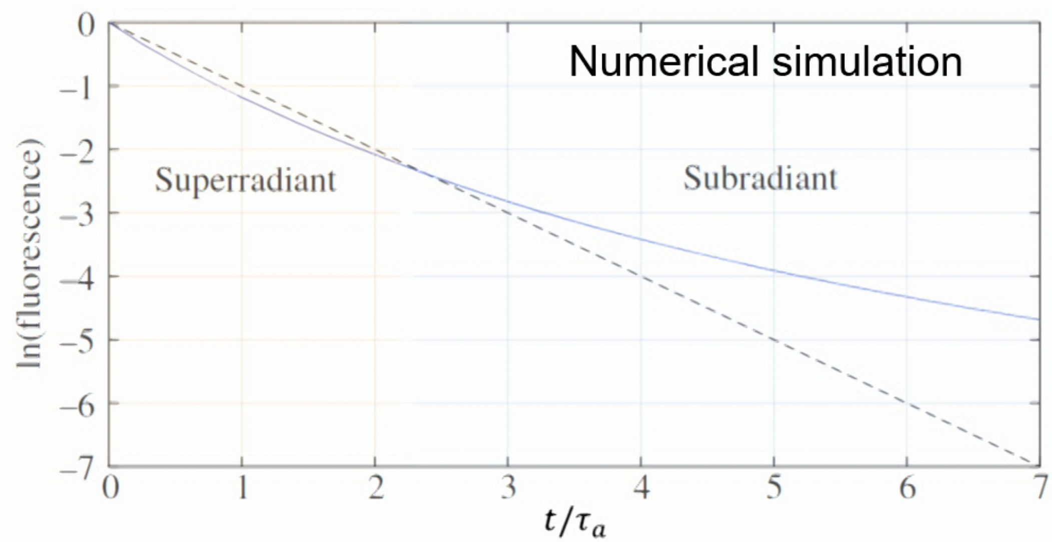

PRX QUANTUM **3,** 010338 (2022)

Spatial Coherence of Light in Collective Spontaneous Emission

D. C. Gold, P. Huft, C. Young, A. Safari, T. G. Walker, M. Saffman, and D. D. Yavuz*

A disordered ensemble of emitters

- An ensemble of atoms can decay superradiantly ($\tau < \tau_a$) or subradiantly ($\tau > \tau_a$) (Dicke, 1954)

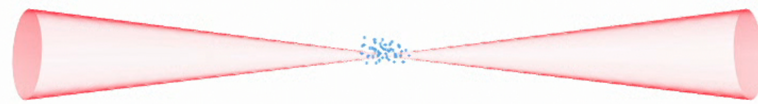

- In a disordered sample in-phase super-radiant modes decay faster, leaving anti-phased sub-radiant modes that are spatially correlated
- The sub-radiant spontaneous emission has spatial coherence, even in a disordered sample, provided the gas is frozen.
- We explore this in the dilute, optically-thin, strong-excitation regime

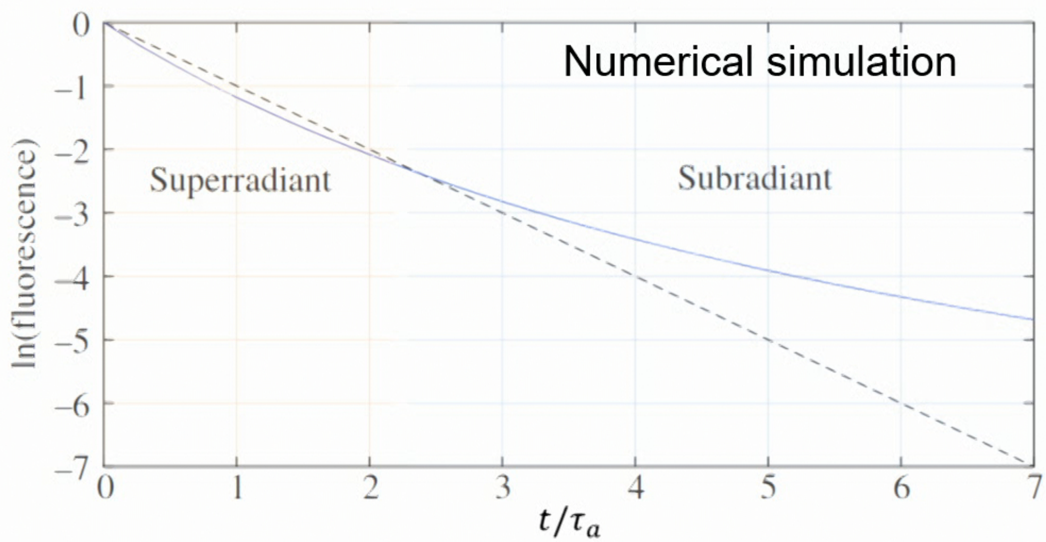

PRX QUANTUM **3,** 010338 (2022)

Spatial Coherence of Light in Collective Spontaneous Emission

D. C. Gold, P. Huft, C. Young, A. Safari, T. G. Walker, M. Saffman, and D. D. Yavuz*

Experiment

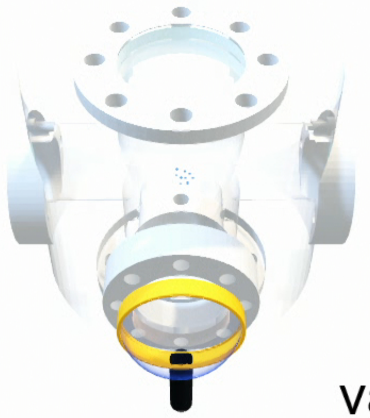

variable expansion time

- MOT is loaded from background ^{87}Rb vapor; sub-Doppler cooling is achieved by detuning MOT lasers (≈40 μK)
- Dipole-trap laser (1064 nm) is focused to 30 microns and overlapped with MOT cloud
- Dipole-trap is turned off, cloud expands for chosen time

Decay curve

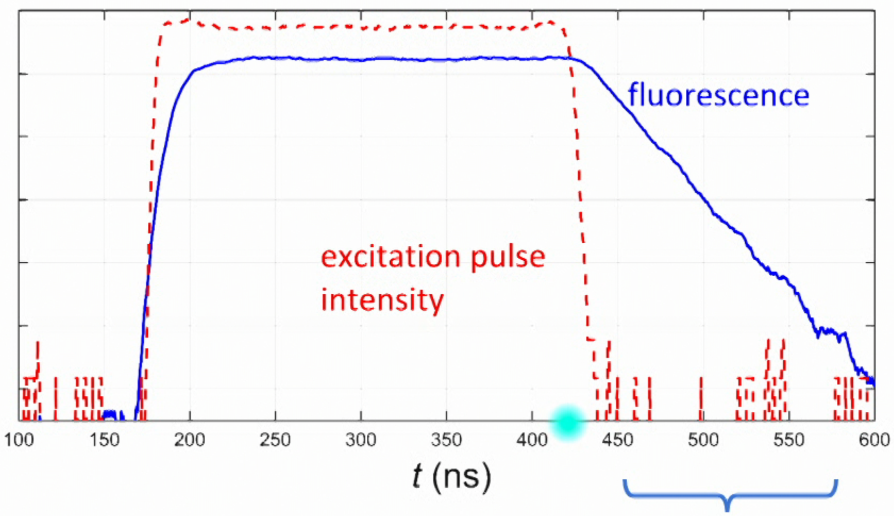
fluorescence
excitation pulse
intensity
100
150
200
250
300
350
400
450
500
550
600
t (ns)

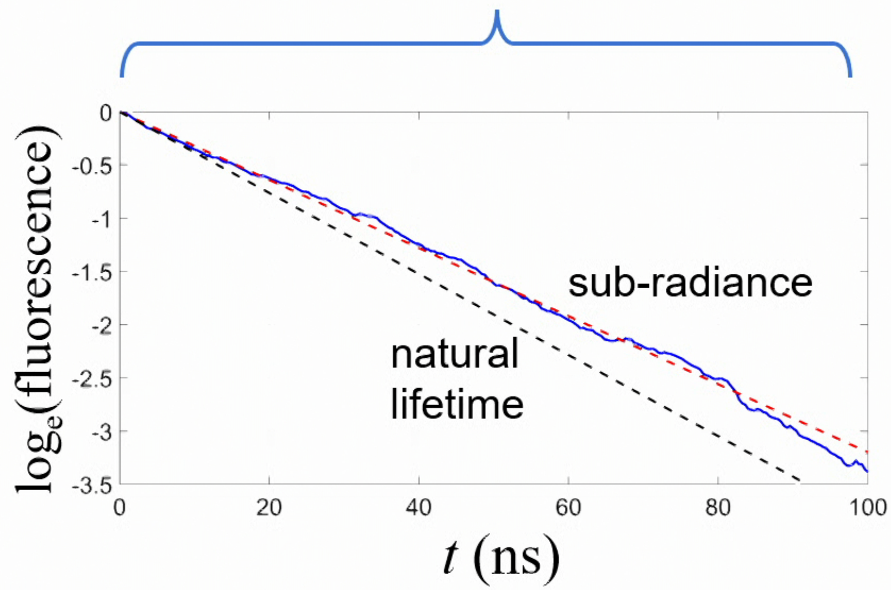
0
-0.5
-1
-1.5
-2
-2.5
-3
-3.5
0
20
40
60
80
100
log_e(fluorescence)
t (ns)
sub-radiance
natural
lifetime

Sub-radiance in dilute limit

11,000 atoms, 30% excitation fraction

Density and optical depth are very small.

Sub-radiance scales with figure of merit for coherent emission

$$[N/(R/\lambda)]^2$$

Incoherent emission scales with o.d.

$$n\sigma R$$

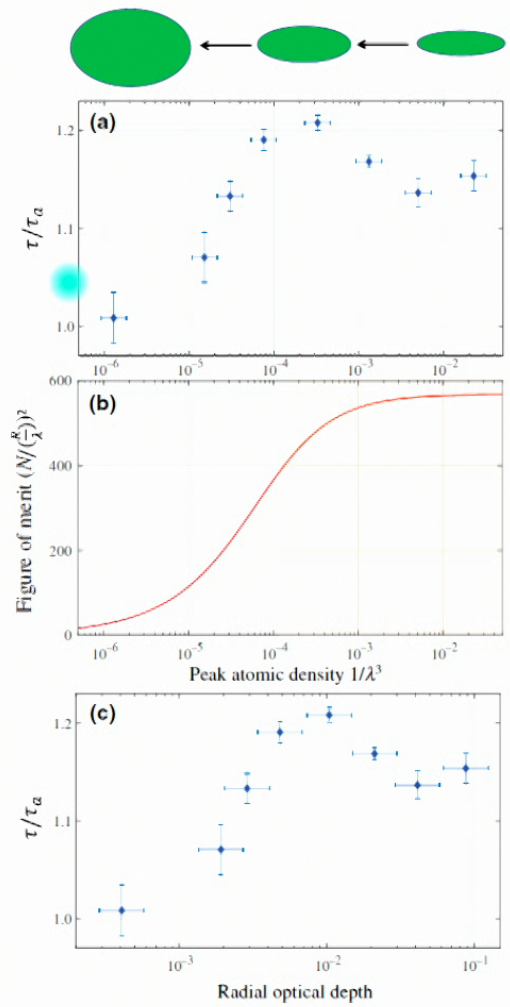

6

Spatial coherence measurements

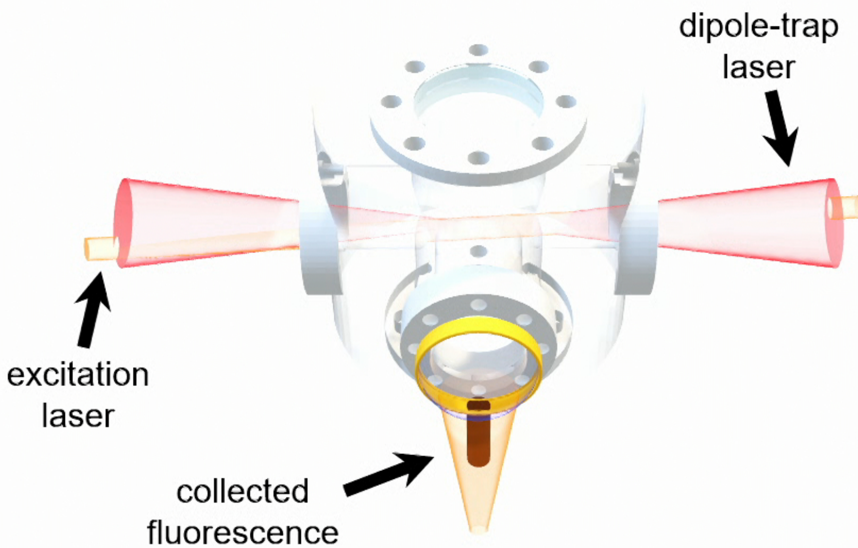

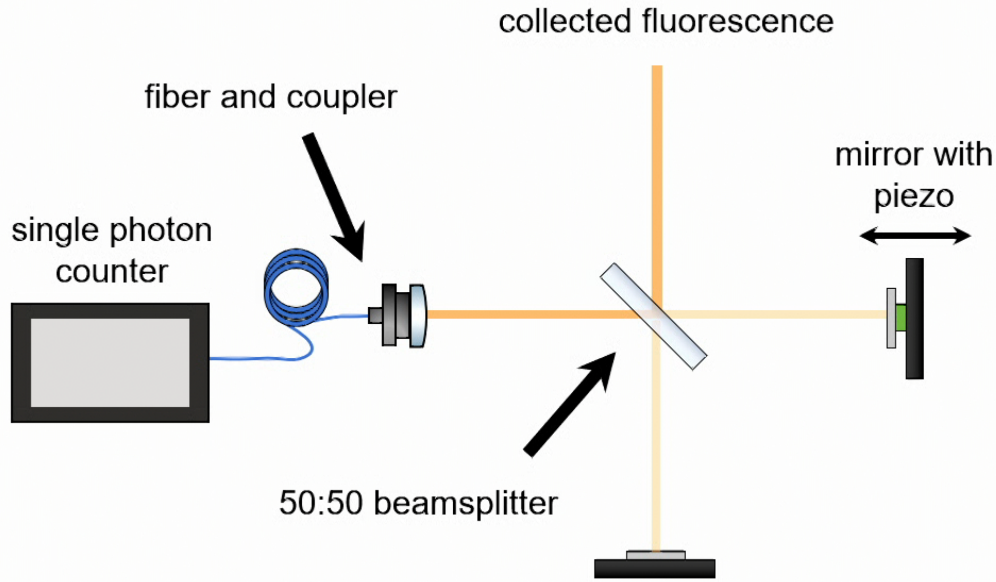

Transverse coherence measurement

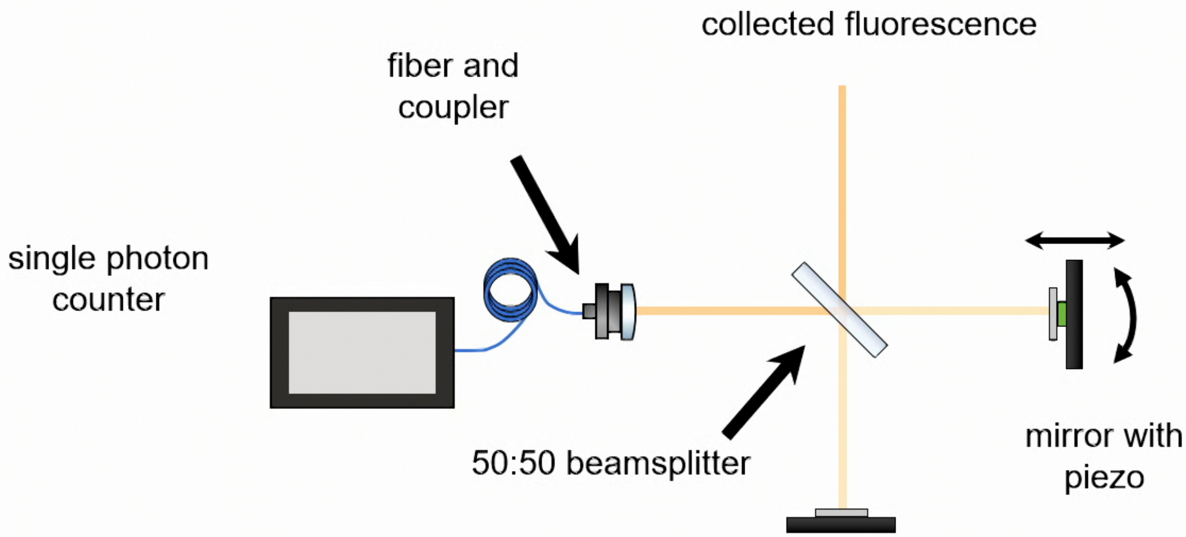

Visibility of coherence

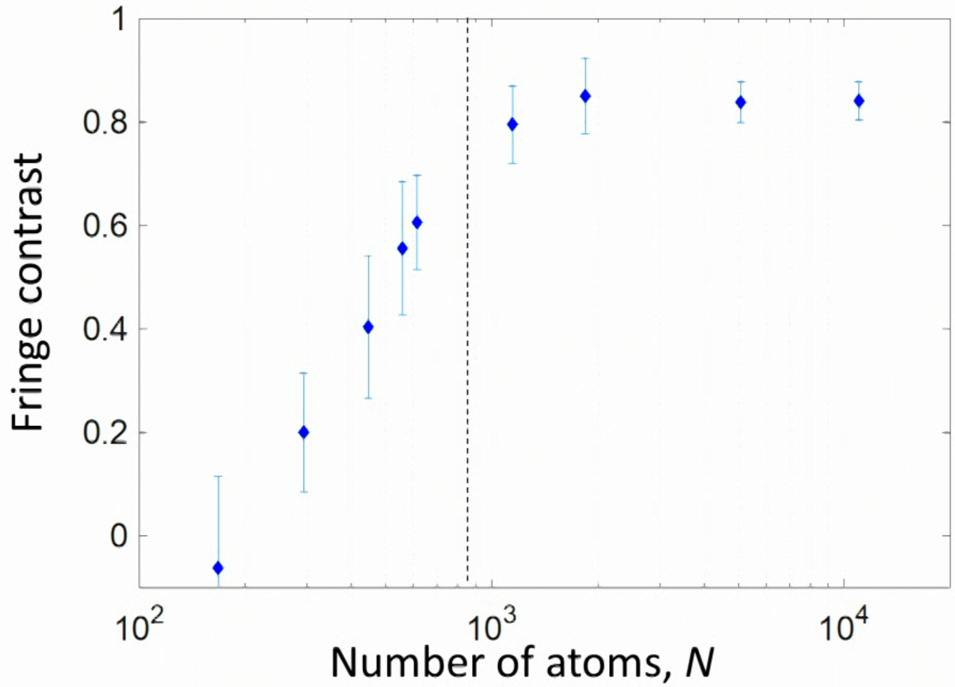

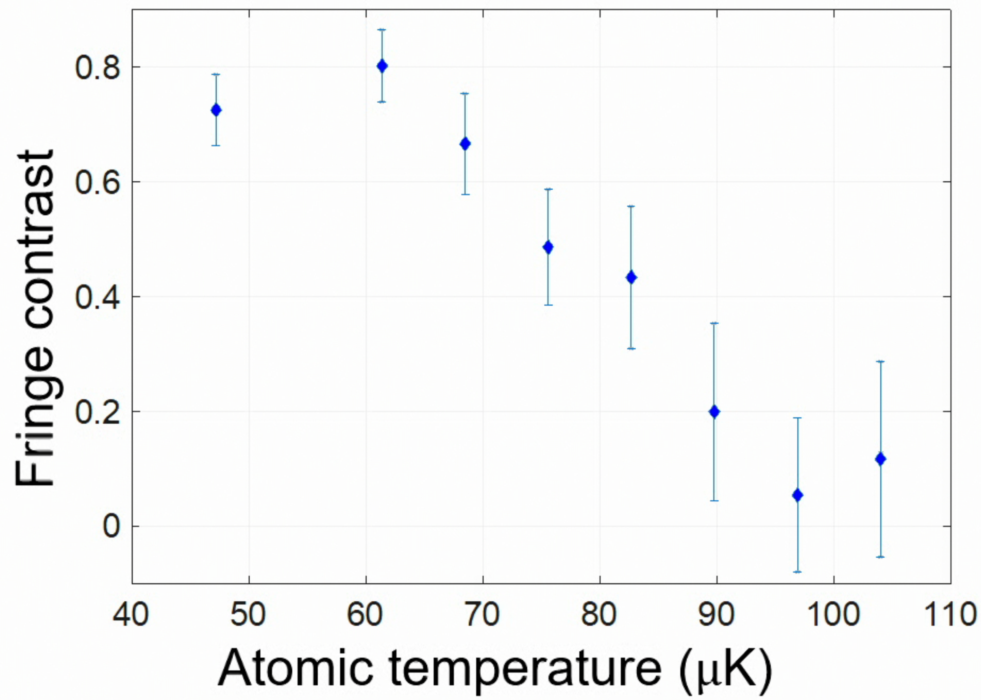

Conclusions / Future directions

- We have observed subradiance in dilute clouds and spatial coherence in collective spontaneous emission.

- Preliminary results that indicate that photon statistics in collective spontaneous emission are non-Poissonian.

- Implications of this result for understanding correlated noise in quantum computers.

Quantum Computing Platforms

trapped ions

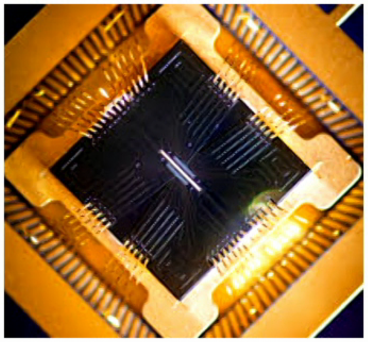

optical

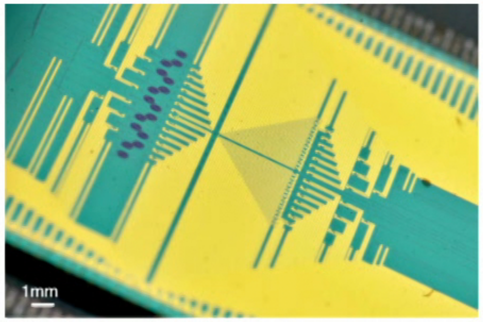

superconductors

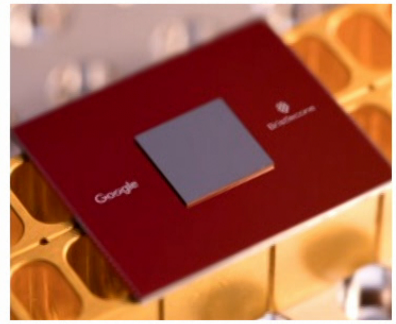

quantum dots

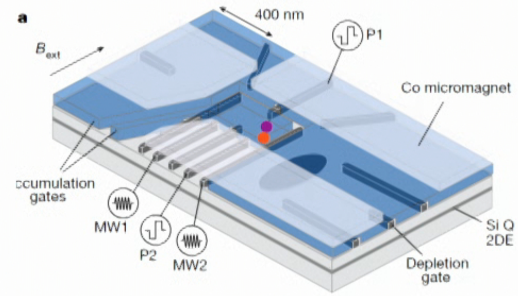

neutral atoms

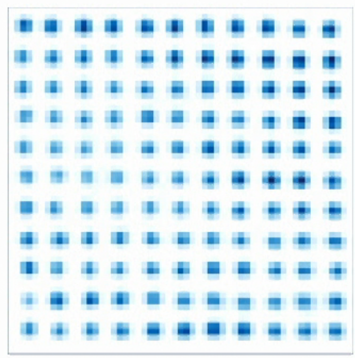

13

The atomic advantage: Isolation & Control

- Laser cooled atoms trapped by light in vacuum.
- Superb quantum memory with coherence from seconds to minutes.
- Selective control using laser pulses
- Excitation of Rydberg state provides super-strong interactions and fast logic operations at tens of nsec.

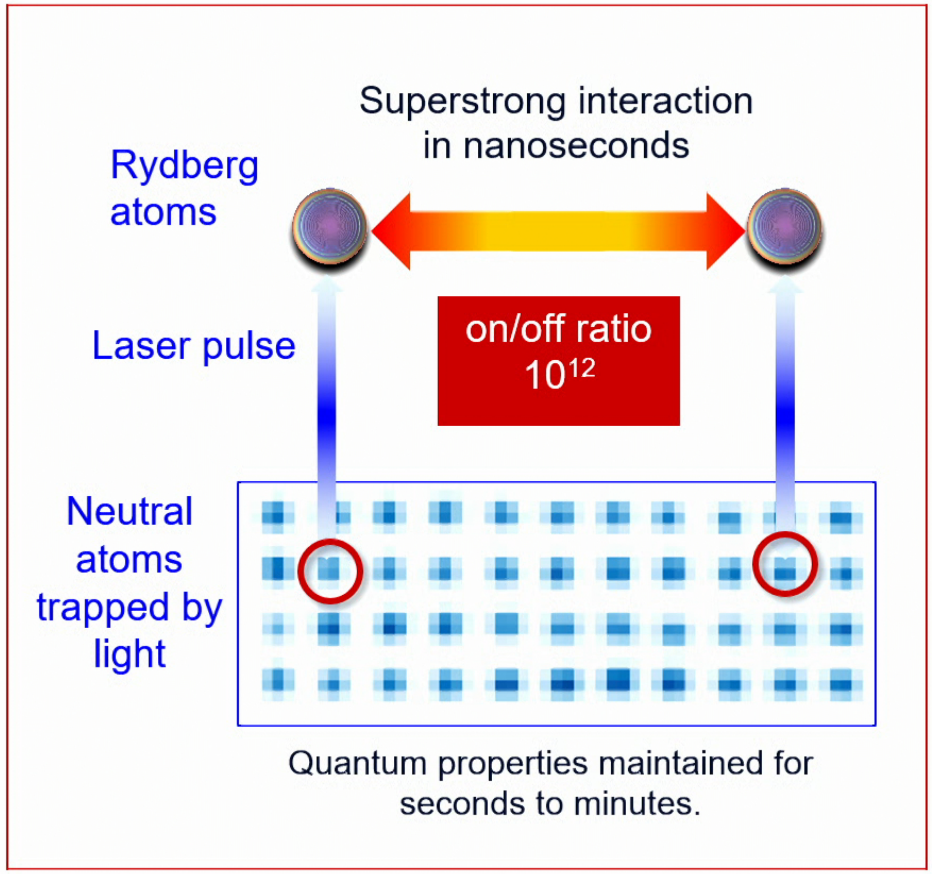

Which atom should we pick ?

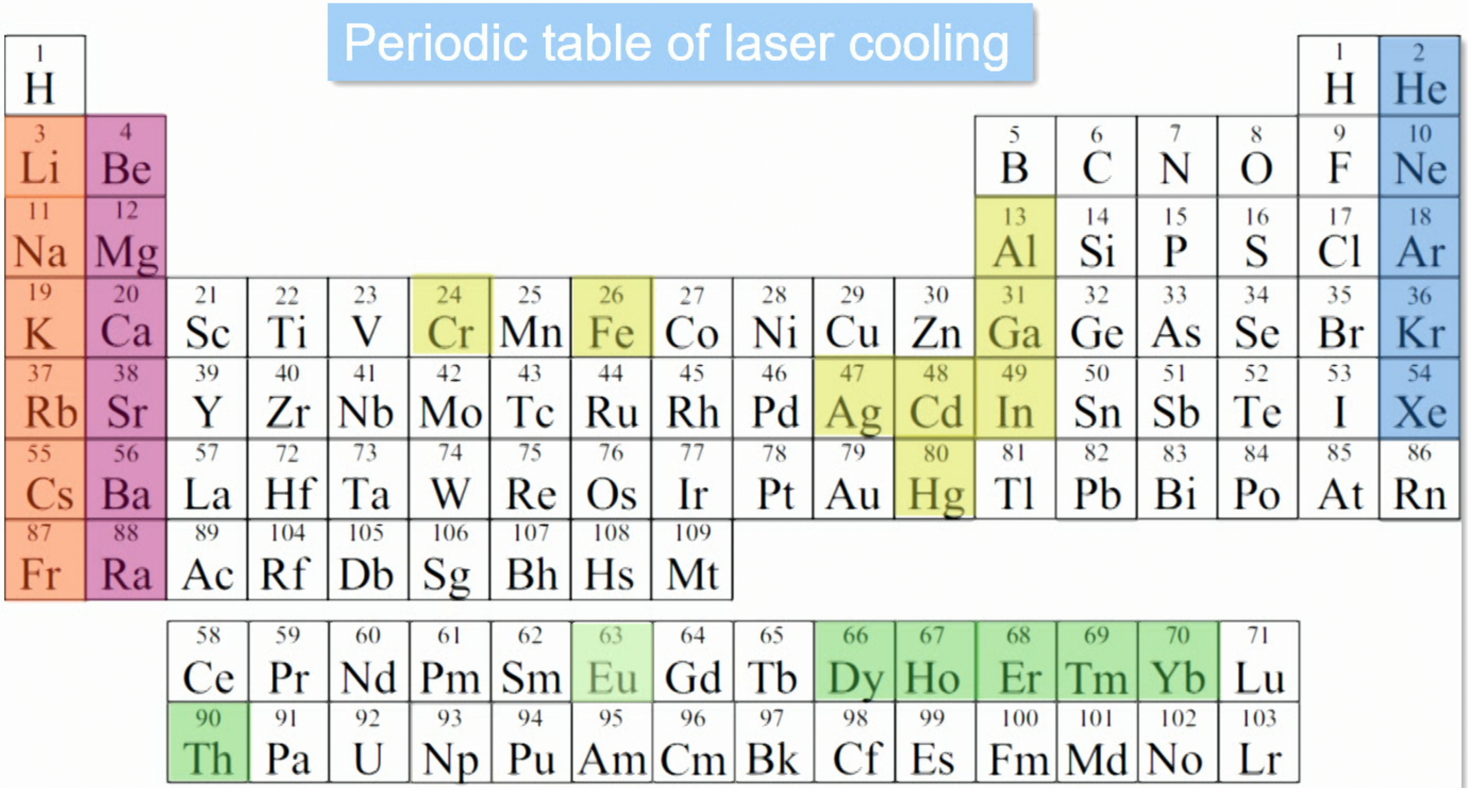

Single atom arrays:

Rb, Cs

Sr, Yb

An industry standard qubit

Cesium

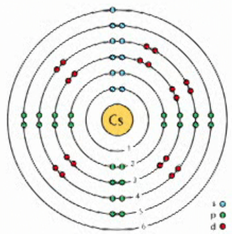

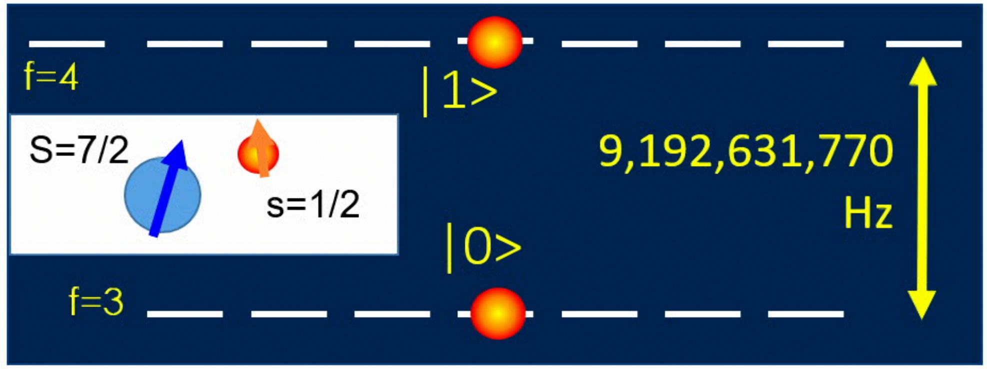

- The hyperfine m=0 clock states provide the SI definition of the second.
- These states are entangled superpositions of nuclear and electronic spin projections

|1>= ↑↓ + ↓↑

|0>= ↑↓ - ↓↑

Excellent coherence properties:

- In free space hyperfine lifetime 34 years
- When optically trapped T1, T2 up to 10s has been demonstrated

Coherence limited by finite atom temperature, trap light optical Stark shifts, magnetic fields.
Minute scale coherence appears possible.

16

Operational Sequence

Qubit Register Preparation

Cold Atoms

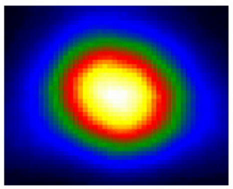

Laser cooling 852,894 nm lasers

Single Atom Array

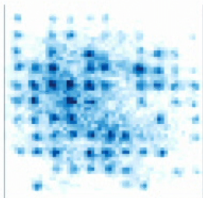

Camera

Array 825 nm lasers, Deep cooling

Filled Array

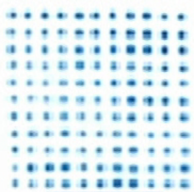

Camera

Rearrange-ment 1064 nm laser

Controlling the Mechanics

Operational Sequence

Qubit Register Preparation

Cold Atoms

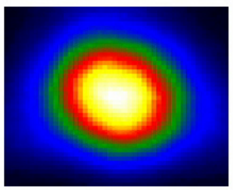

Laser cooling 852,894 nm lasers

Single Atom Array

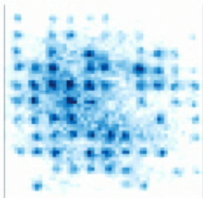

Camera

Array 825 nm lasers, Deep cooling

Filled Array

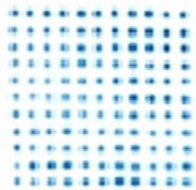

Camera

Rearrange-ment 1064 nm laser

Controlling the Mechanics

Calculation Cycle

State Initialization

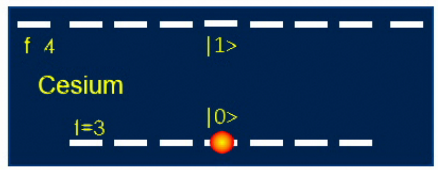

Optical Pumping 895 nm laser

Quantum Circuit

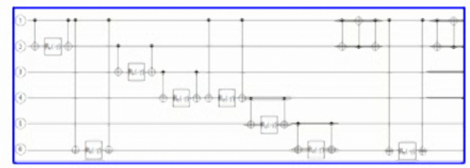

Gates 1Q, 2Q 459 nm, 1040 nm lasers, μwaves

Measure Results

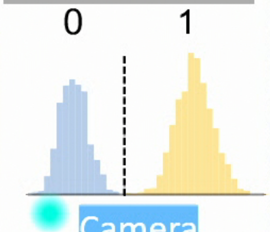

Camera

852 nm lasers

Controlling the Quantum

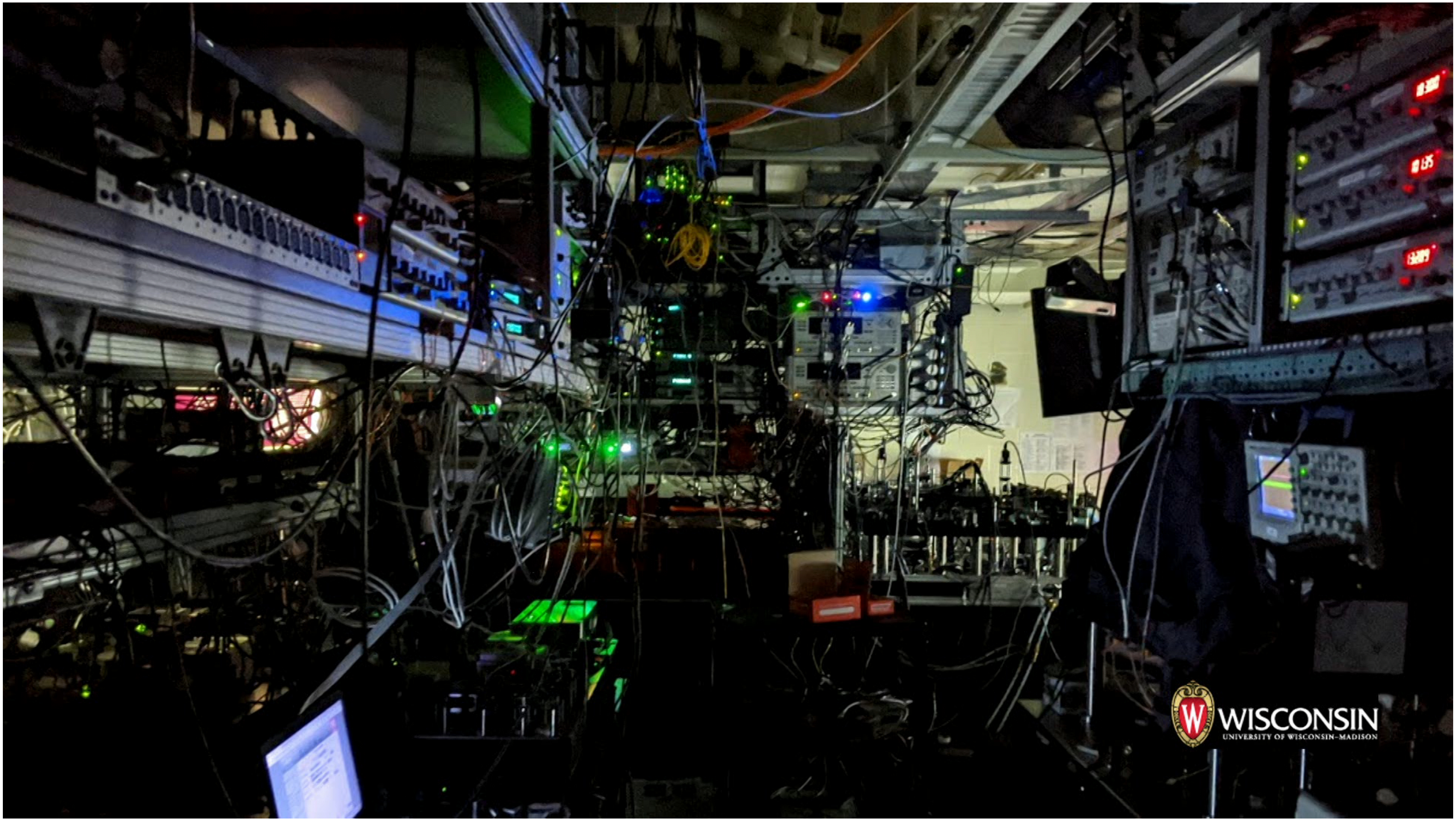

Experimental geometry

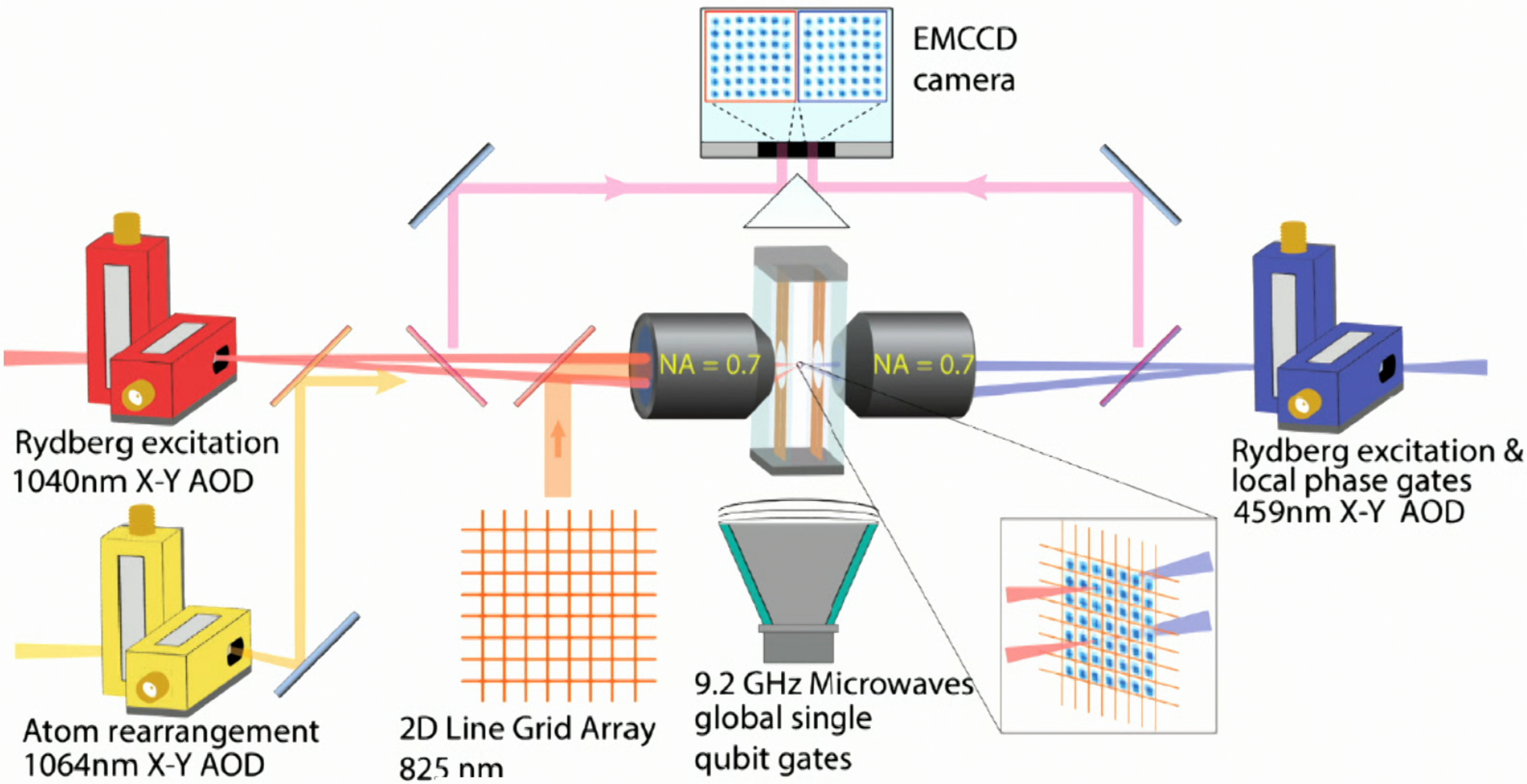

Laser auto relock

System auto relocks Rydberg laser to correct ULE mode.

Diagnostics:

- ULE transmission
- Transverse mode
- Low resolution wavemeter

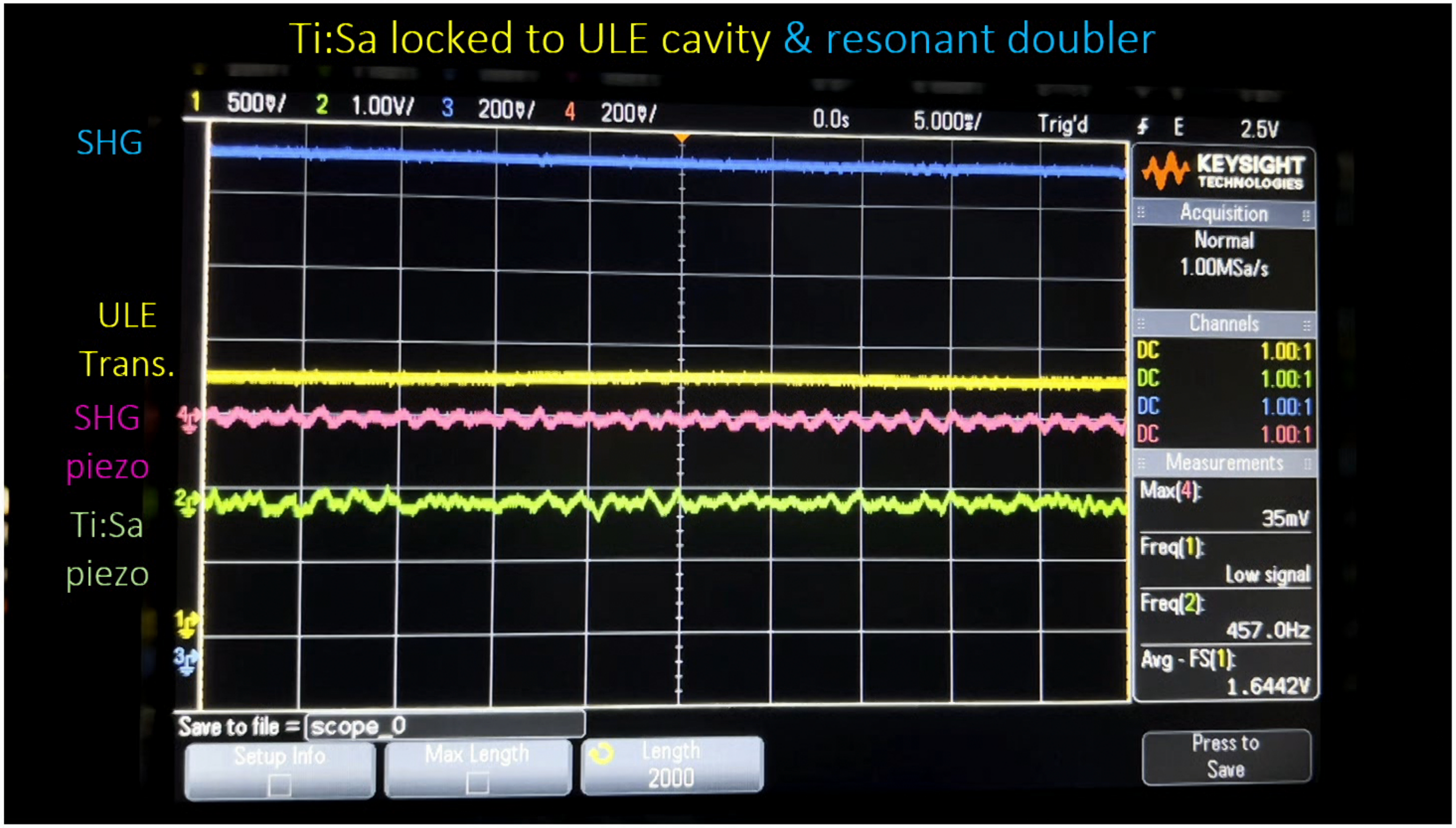

Jacob Abraham

Scott

Gate set

Encode in Cs clock states:

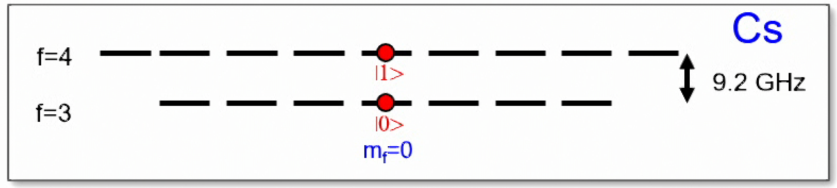

Bias field of 1.5 G

Universal gate set:

Global gates
microwaves

$$\prod_{sites} R_\varphi(\theta)$$

Angle ϕ in x-y plane
from μwave phase

Rydberg gate

$$C_Z(i,j)$$

i,j site indices $|i-j| \leq 3$ or more

Single site gates
microwaves+optical
Stark shift

$$R_\varphi(\theta)$$

Rydberg gate &
local rotations

$$C_X(i,j)$$

Native multi-qubit gates are also possible: $(CNOT)^k$, C_kNOT.
Harvard Toffoli demonstration.

Single qubit gates - global

PRL 114, 100503 (2015)

Cs clock state qubits

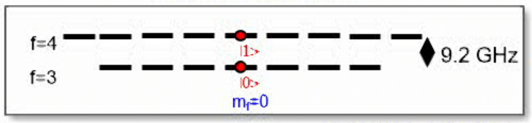

Bias field of 1.5 G

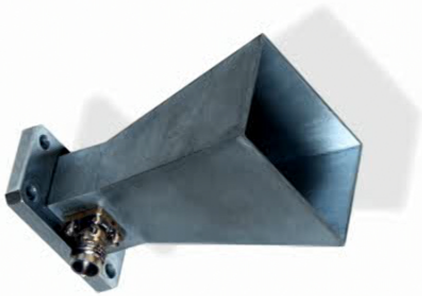

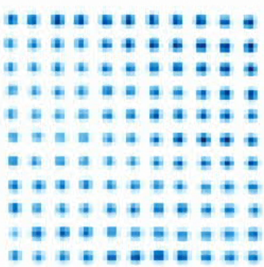

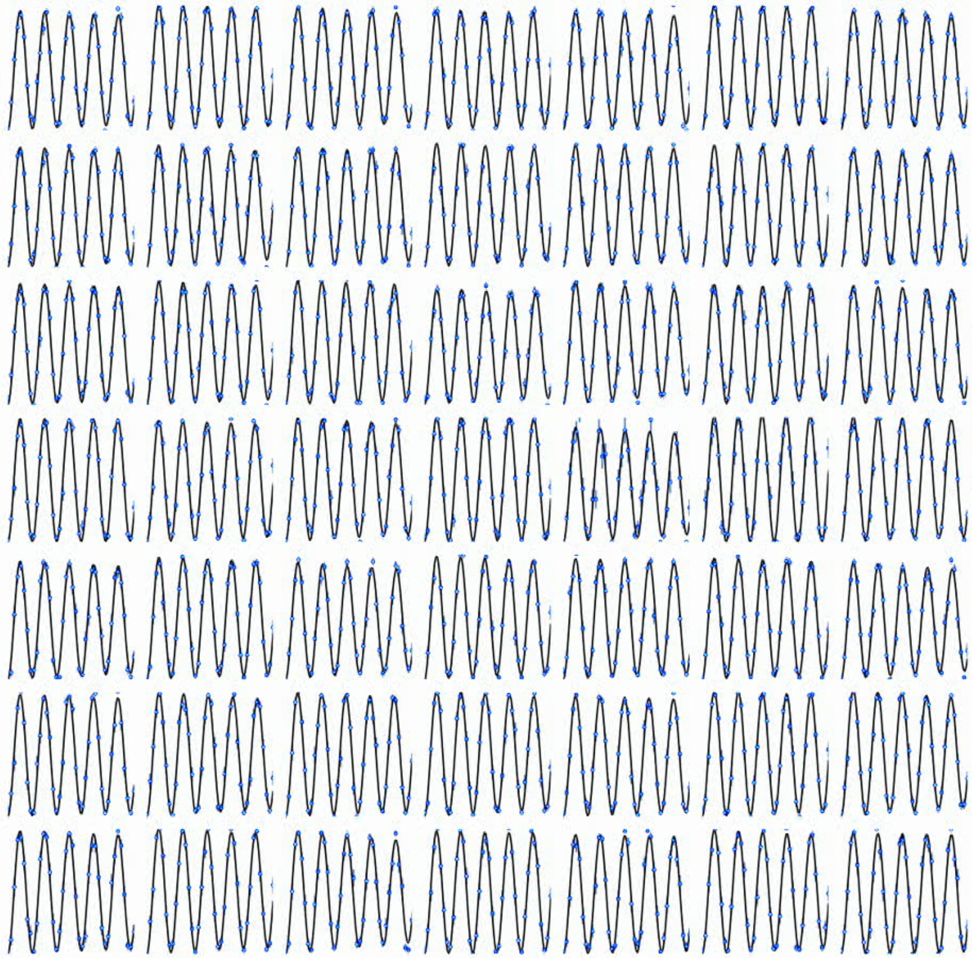

Microwaves 10 kHz Rabi frequency

$\langle F^2 \rangle_{47\ \mathrm{sites}}$	0.9983 ± 0.0014
F^2_{min}	0.9939 ± 0.0007
F^2_{max}	0.9999 ± 0.0003

Single qubit site selected gates

A $R_z(\theta)$ gate is obtained with a focused Stark shift laser.

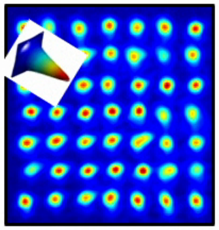

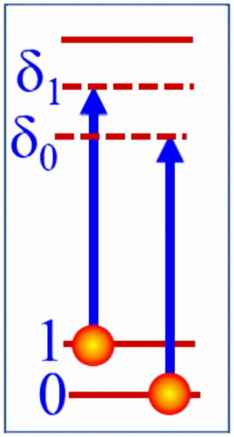

Single qubit gates – local Randomized Bencharking

SPAM 6 sites

Average error=0.025

Extracted from local RB

Local gates 6 sites

average F=0.993

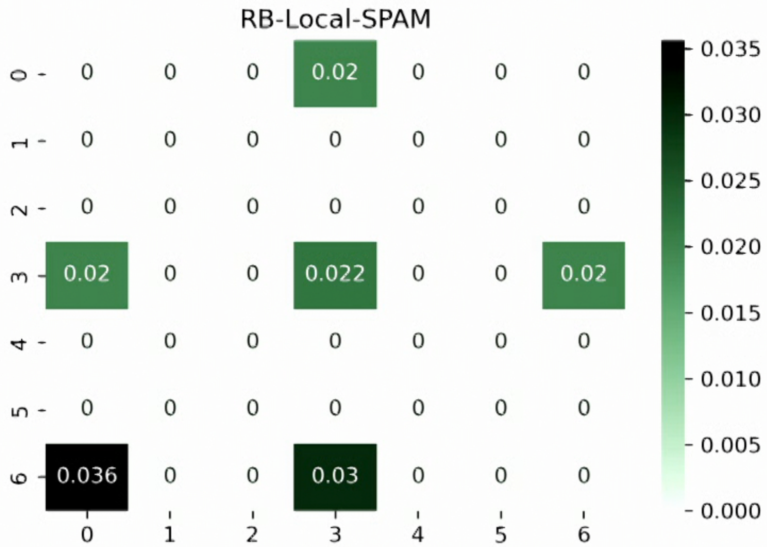

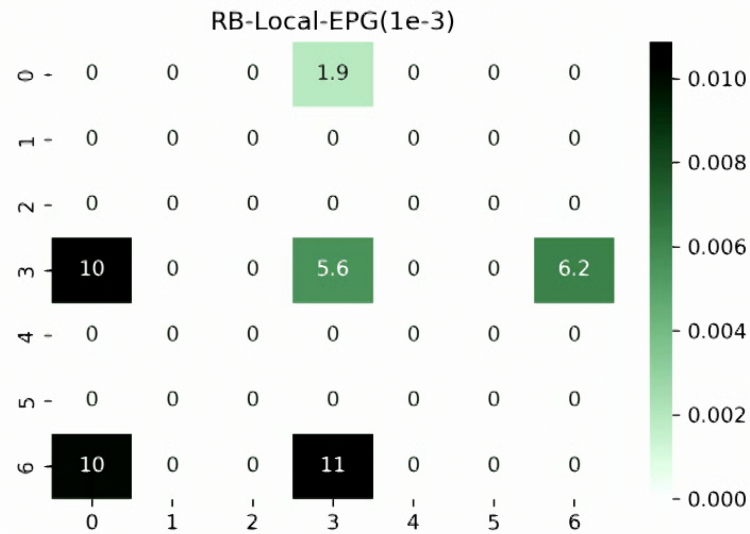

Optical addressing

- Focused Gaussian control beams with w=3 μm
- Very sensitive to alignment

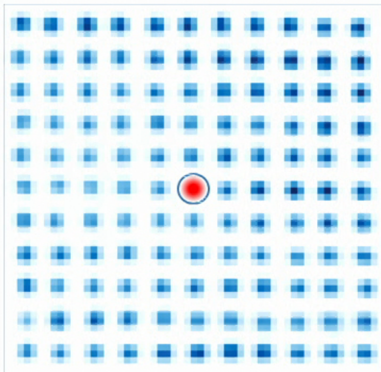

Simulated Rz error

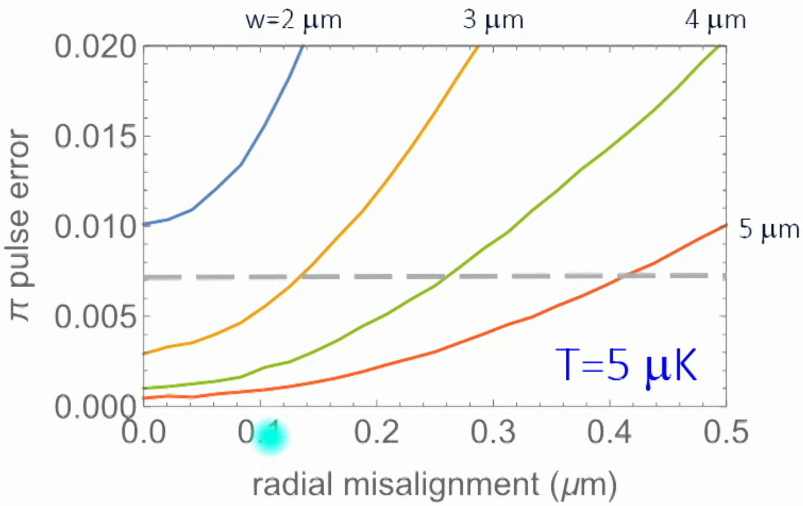

Measured beam position jitter

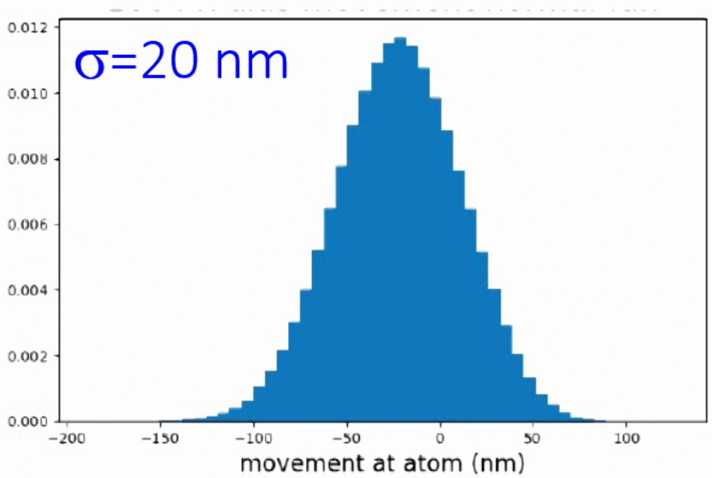

2Q gate fidelity

- Rydberg 75s state
- Small beams w=3 μm for individual qubit addressing
- Used protocol from Levine, et al. (2019) with parameters adjusted for both strong and weak blockade.
- SPAM corrected Bell fidelity F~0.955.

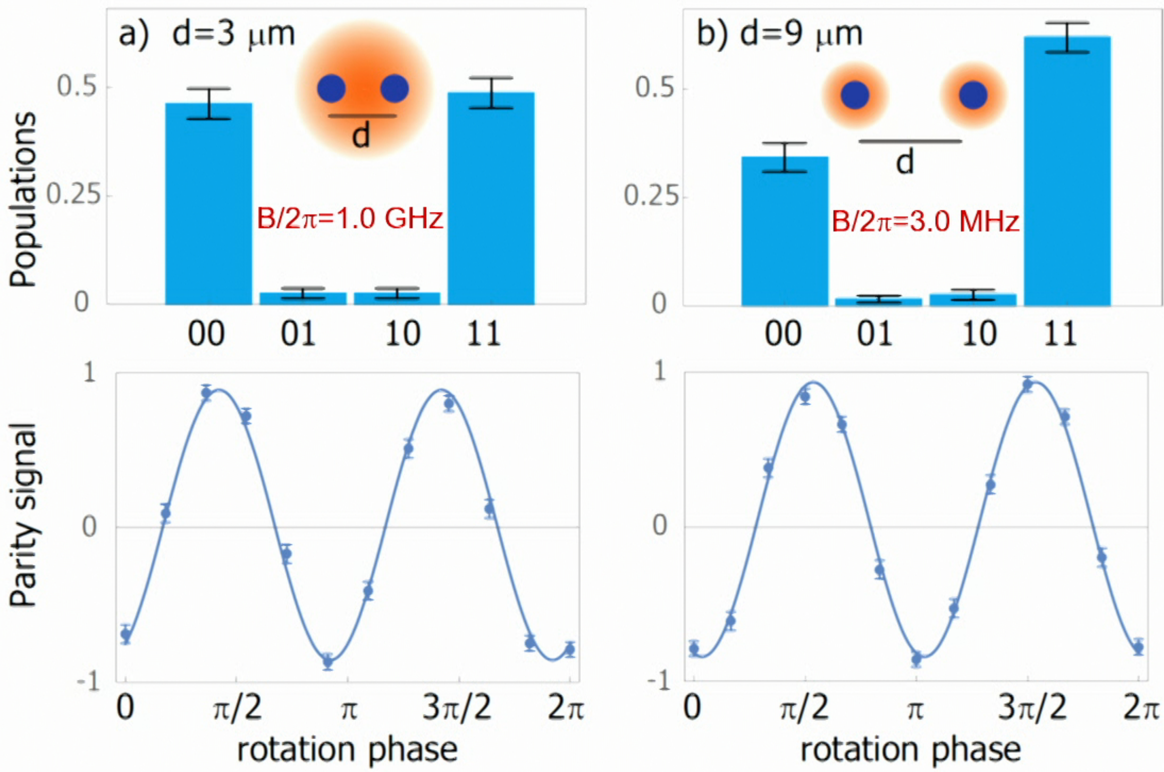

FIG. SM-9: Characterization of $\mathsf{C_Z}$ gate fidelity be preparation of Bell states. a) Two qubits spaced by $d = 3\ \mu$m addressed with large beams of waist $w = 7.5\ \mu$m focused halfway in between the qubits. At $d = 3\ \mu$m there is a strong blockade of $\mathsf{B}/2\pi = 1.03$ GHz. Measured values were $P_{\rm Bell} = 0.475(0.01)$, parity amplitude $C = 0.440(0.01)$ and fidelity $F_{\rm Bell} = 0.914(0.014)$. b) Two qubits spaced by $d = 9\ \mu$m addressed with separate beams with waist $w = 3\ \mu$m. At this spacing the blockade is weak, $\mathsf{B}/2\pi = 3.0$ MHz. Measured values were $P_{\rm Bell} = 0.483(0.009)$, parity amplitude $C = 0.444(0.010)$ and fidelity $F_{\rm Bell} = 0.927(0.013)$.

Quantum circuits with neutral atom qubits

Stationary control beams / moving atoms

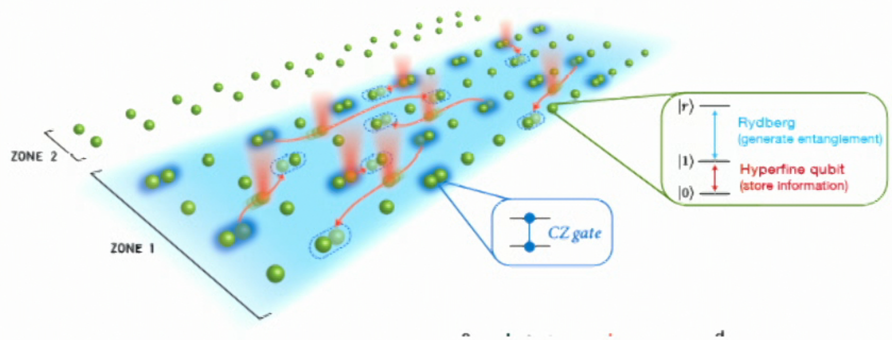

Harvard/MIT
Nature **604**, 451 (2022)

Moving control beams / stationary atoms

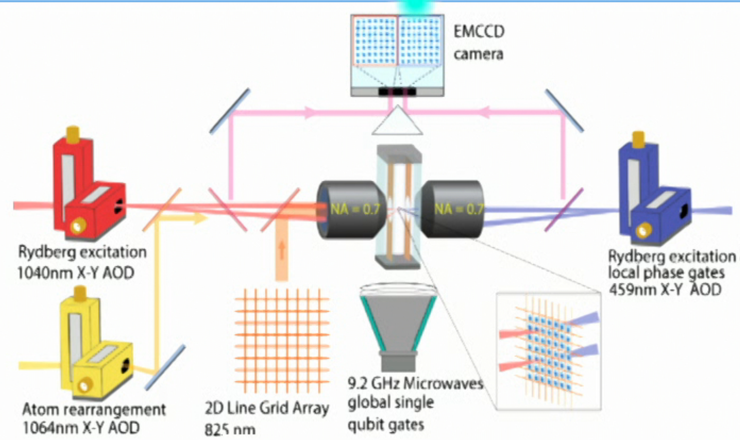

Wisconsin/ColdQuanta
Nature **604**, 457 (2022)

GHZ states

- A good test of circuit operation is preparation of entangled GHZ states

$$|GHZ\rangle_N = \frac{|00\ldots0\rangle + |11\ldots1\rangle}{\sqrt{2}} = \frac{|0^{\otimes N}\rangle + |1^{\otimes N}\rangle}{\sqrt{2}}$$

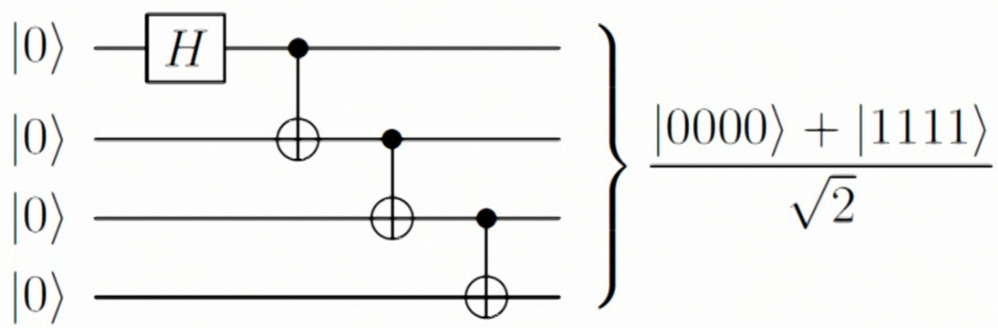

Phase estimation

- Quantum phase estimation is one of the most important quantum algorithms. Useful for quantum chemistry and factoring.

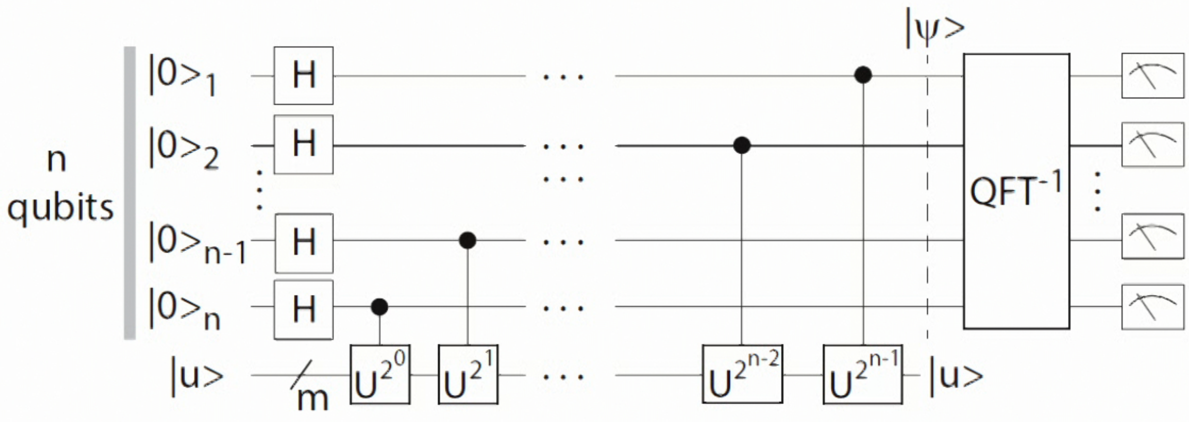

Figure 4.9: Circuit for finding the phase of the unitary operator U. The notation $/_m$ means a bundle of m qubits. The size m of the second register is chosen to be large enough to hold $|u\rangle$.

Phase estimation

- Test for measuring phases of $0, \pi/2, \pi, 3\pi/2$

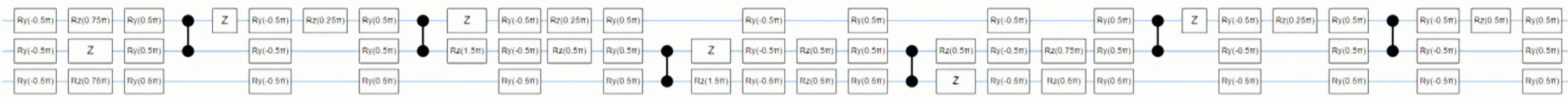

Output register

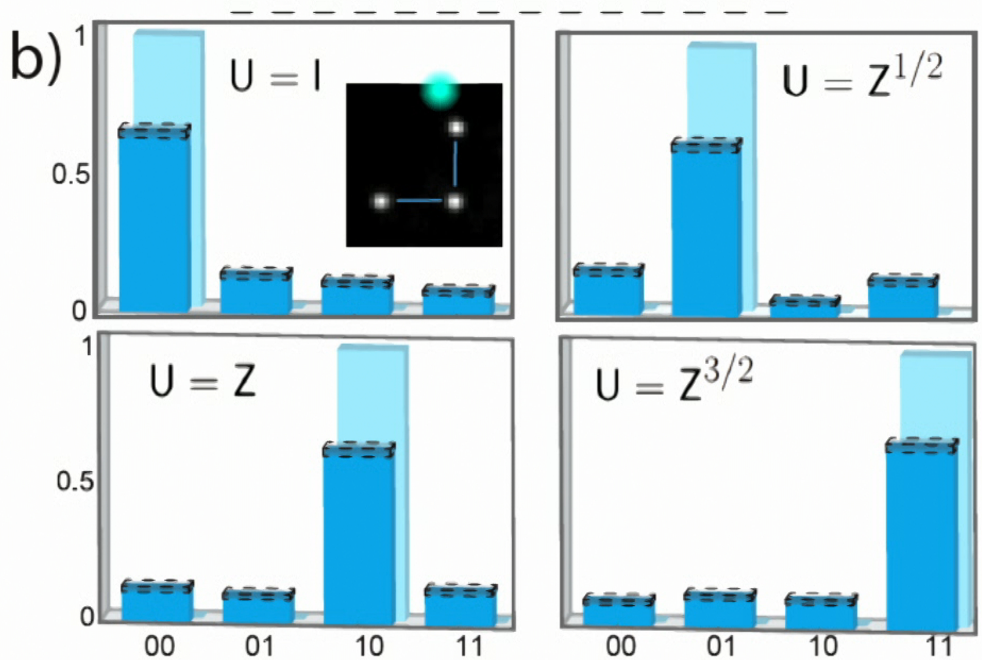

Quantum phase estimation – Hydrogen molecular energy

- Hydrogen molecular Hamiltonian

$$\hat{H} = \sum_{i,j} h_{ij} \hat{a}_i^\dagger \hat{a}_j + \frac{1}{2} \sum_{i,j,k,l} h_{ijkl} \hat{a}_i^\dagger \hat{a}_j^\dagger \hat{a}_k \hat{a}_l$$

h_{ij}, h_{ijkl}: numerical value (STO-3G basis)

4 electronic orbitals

QAOA MaxCut

NP-complete graph partioning problem.

QAOA applies *p* rounds of cost function and mixing operators with adjustable weights.

$$\hat{H}_Z = \sum_{(n,m)\in E} \frac{1}{2}\left(\hat{Z}_n \hat{Z}_m - \hat{\mathbb{I}}\right)$$

p=3 circuit
43 single qubit gates
18 CZ gates

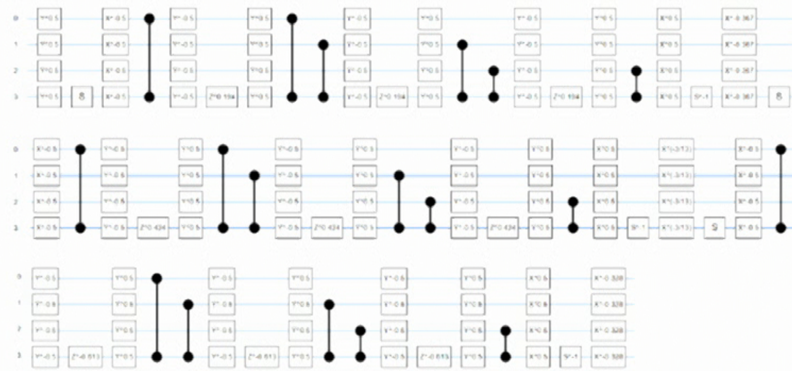

Ideal circuit: $R_a = 0.772$ 0.934 1.0

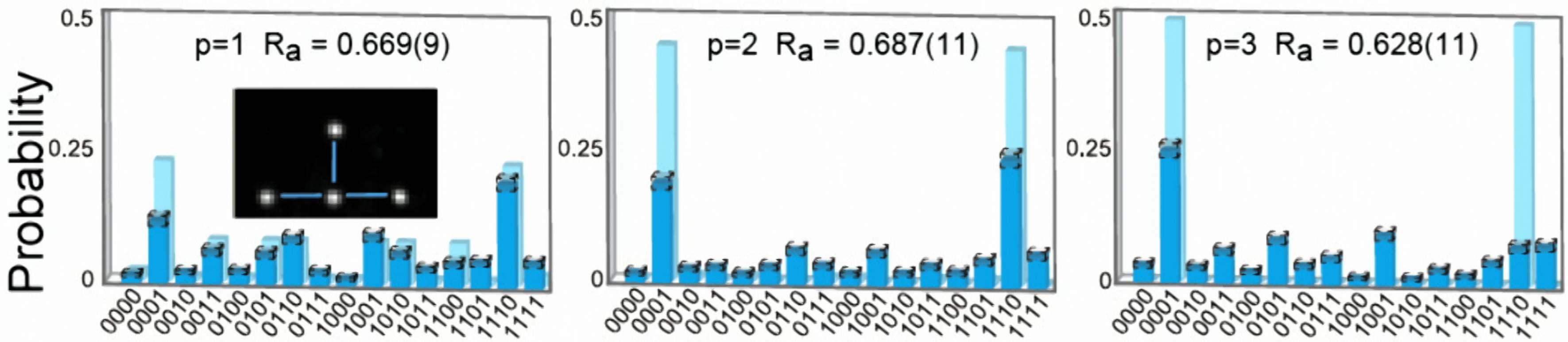

QAOA MaxCut – Quantum Advantage ?

- Heuristic classical solvers provide high quality solutions rapidly on large graphs.
- Extensive numerics show quantum advantage for 3-regular graphs requires noiseless execution of p>11 circuits.
- Quantum advantage appears unlikely for 3-regular graphs without error correction.
- Pre-error correction quantum advantage may exist for other problems.

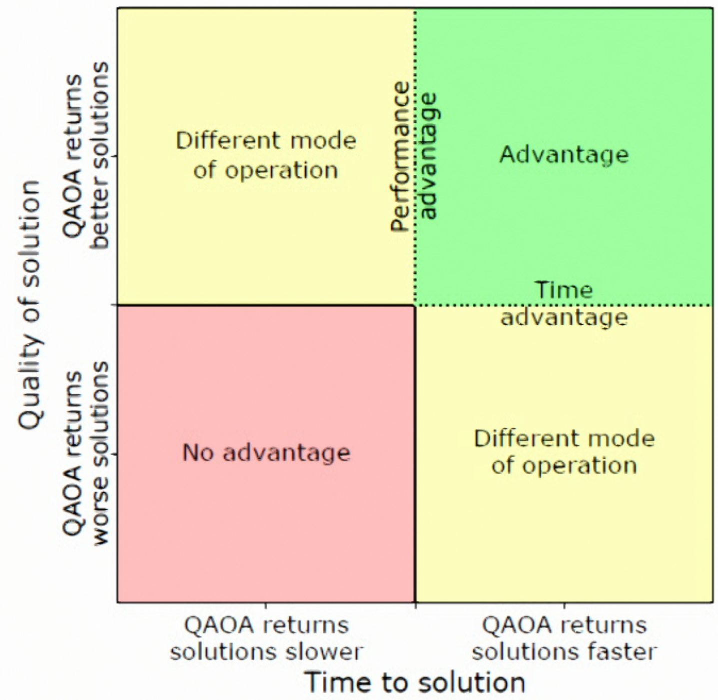

arXiv:2206.03579

Sampling Frequency Thresholds for Quantum Advantage of Quantum Approximate Optimization Algorithm

Danylo Lykov,[1,2,*] Jonathan Wurtz,[3,4] Cody Poole,[5,†] Mark Saffman,[5,6,‡] Tom Noel,[7,§] and Yuri Alexeev[1,¶]

Outlook

- The full potential of quantum computing will require error correction for fault tolerance.
- Quantum error correction is VERY resource demanding.
- Depending on the coherence of the qubits and the fidelity of gate operations and measurements a fault tolerant logical qubit may require 100 – 1000 physical qubits
- Thus a machine with 100 logical qubits may need 10^4 or more physical qubits

More qubits

Phys. Rev. A **105**, 063111 (2022)

4f filtering

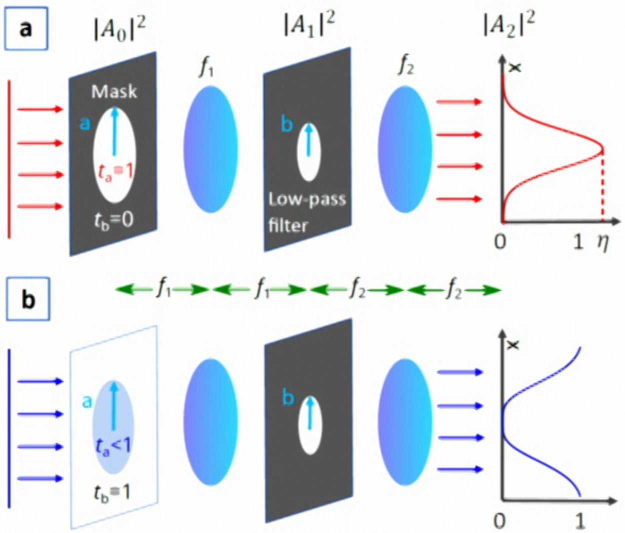

A simple, passive design for large optical trap arrays for single atoms

P. Huft,[1] Y. Song,[1] K. Jooya,[1] T. M. Graham,[1] S. Deshpande,[2] C. Fang,[2] M. Kats,[2] and M. Saffman[1,3]

More qubits

Phys. Rev. A **105**, 063111 (2022)

4f filtering

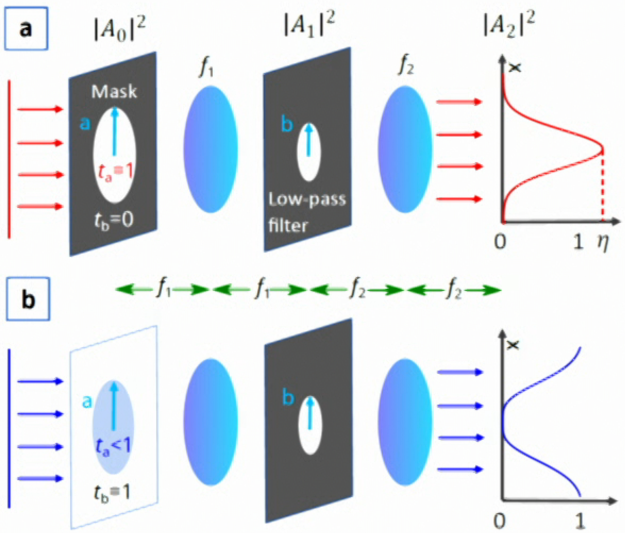

A simple, passive design for large optical trap arrays for single atoms

P. Huft,[1] Y. Song,[1] K. Jooya,[1] T. M. Graham,[1] S. Deshpande,[2] C. Fang,[2] M. Kats,[2] and M. Saffman[1,3]

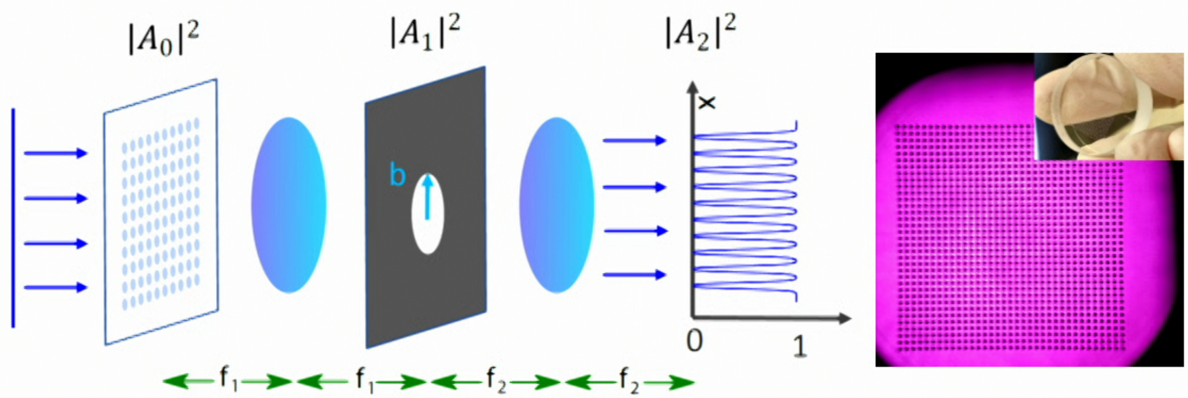

More qubits

Phys. Rev. A **105**, 063111 (2022)

4f filtering

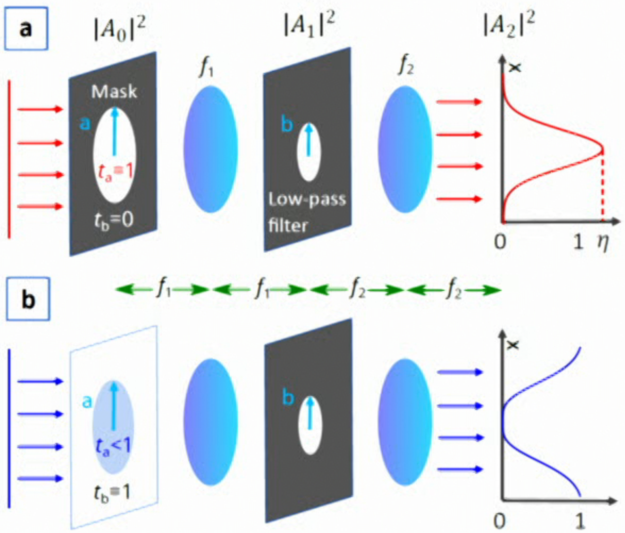

A simple, passive design for large optical trap arrays for single atoms

P. Huft,[1] Y. Song,[1] K. Jooya,[1] T. M. Graham,[1] S. Deshpande,[2] C. Fang,[2] M. Kats,[2] and M. Saffman[1,3]

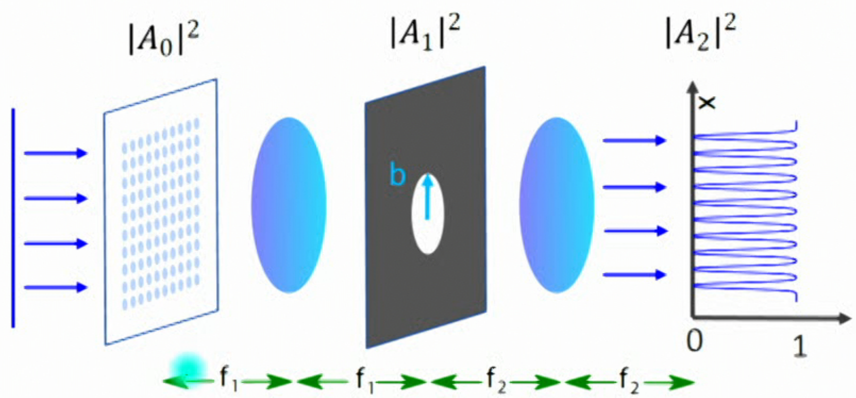

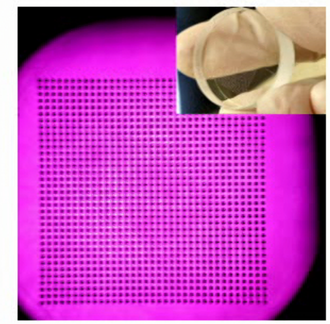

Single shot average image atom histograms

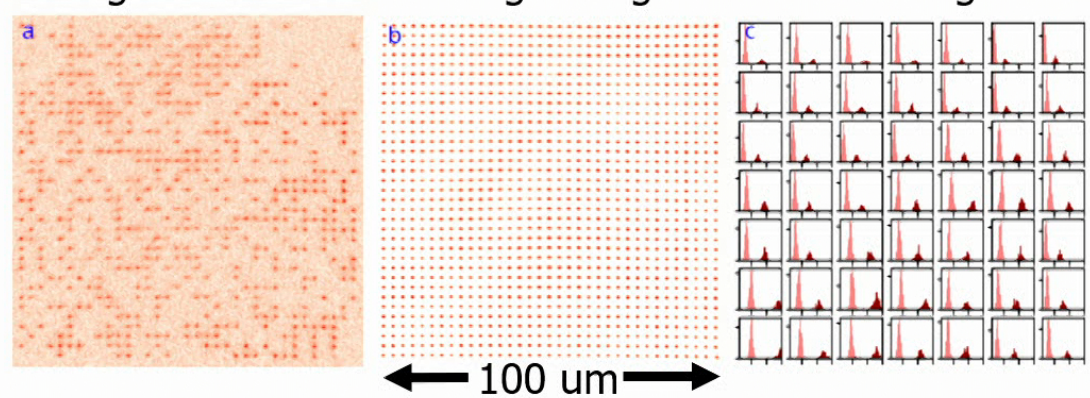

Array of 1225 blue traps for Cs atoms

Low cost, multimode laser.

Can be scaled to thousands

Rydberg entanglement experiments

	Wisconsin	Harvard	Wuhan	Caltech
Architecture	2D array, blue traps, focused beams 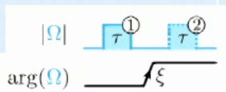	2D array, red traps, large beams 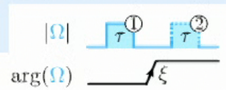	2D array red traps, medium size beams 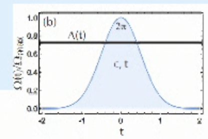	1D array, red traps, large beams
Atom	Cs	87Rb	87Rb	Sr
2Q Bell state fidelity Raw (-SPAM)	0.955 (>0.965)	0.95 (0.97)	0.95 (0.98)	0.98(0.991)
Notes	Ti:Sa lasers "Pichler" 2-pulse protocol	Ti:Sa lasers "Pichler" 2-pulse protocol	Filtered diode lasers Adiabatic 1-pulse protocol	Ground-Rydberg qubit, short lived
Papers	Nature **604**, 457 (2022)	Nature **604**, 451 (2022)	https://arxiv.org/abs/2109.02491 PRA **103**, 022424 (2021)	Nat. Phys. 16, 857 (2020)

Rydberg entanglement experiments

	Wisconsin	Harvard	Wuhan	Caltech
Architecture	2D array, blue traps, focused beams 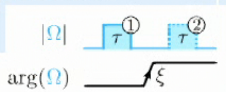	2D array, red traps, large beams 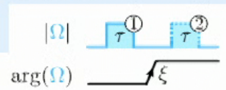	2D array red traps, medium size beams 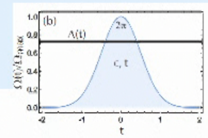	1D array, red traps, large beams
Atom	Cs	87Rb	87Rb	Sr
2Q Bell state fidelity Raw (-SPAM)	0.955 (>0.965)	0.95 (0.97)	0.95 (0.98)	0.98(0.991)
No				g
Pa				

F_{raw}=0.955

F_{-SPAM}>0.965

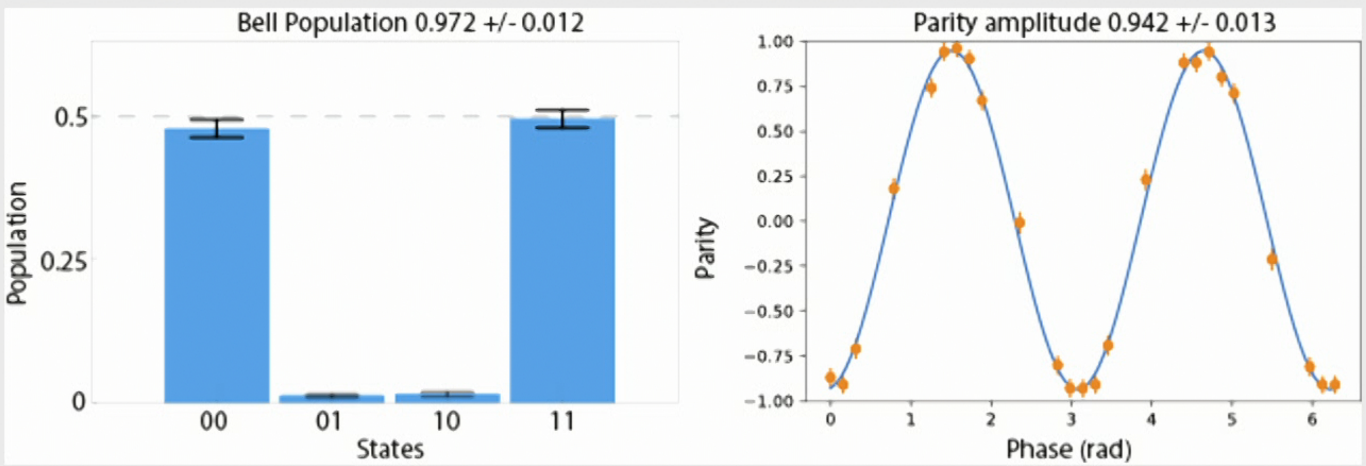

Gate fidelity outlook

Performance drivers:

- Stable optomechanics
- Colder atoms/tight confinement
- Smooth optical spatial profile
- Lower laser noise
- Stabilized E field environment
- Automated tuning system
- Robust protocols

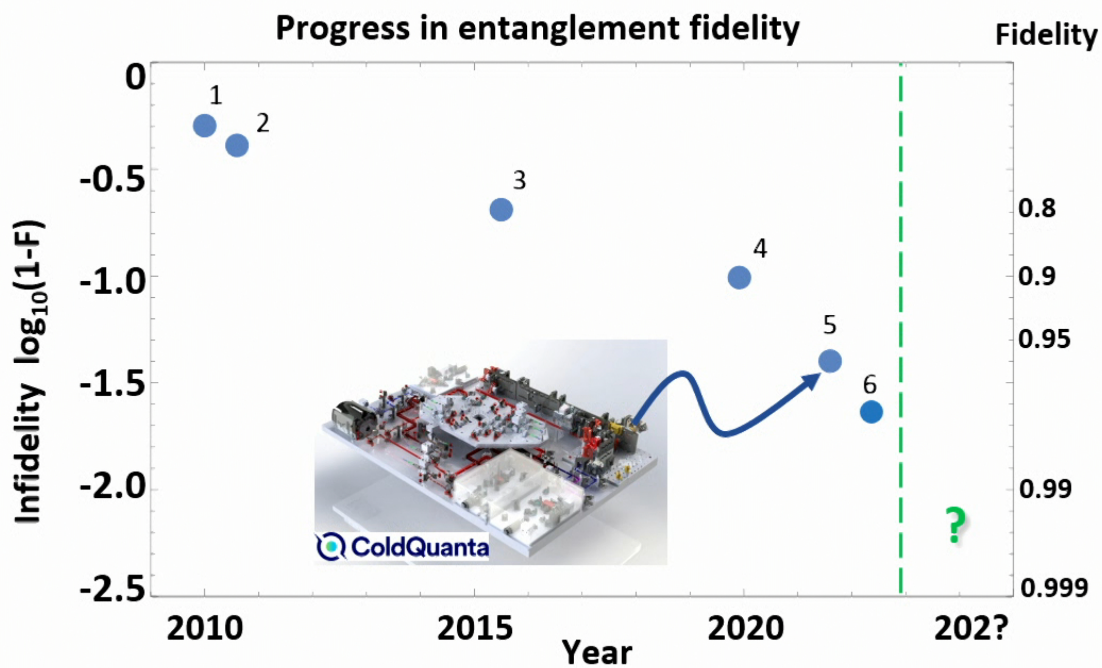

UWM results: (1) First neutral atom CNOT: PRL **104**, 010503(2010), (2) PRA **82**, 030306(R) (2010)
(3) PRA **92**, 022336 (2015), (4) PRL **123**, 230501 (2019), (5) Nature **604**, 457 (2022), (6) F_{Bell}=0.965 [unpublished] (2022)

Midcircuit measurements

WORK IN PROGRESS

For error correction need measurements on a subset of qubits, without disturbing data qubits

- Shelve non-measured qubits in f=3
- Transfer 4,0 state of measured qubits to 4,4
- Measure by cycling 4,4 <-> 5,5
- Recool and restore atom to qubit basis

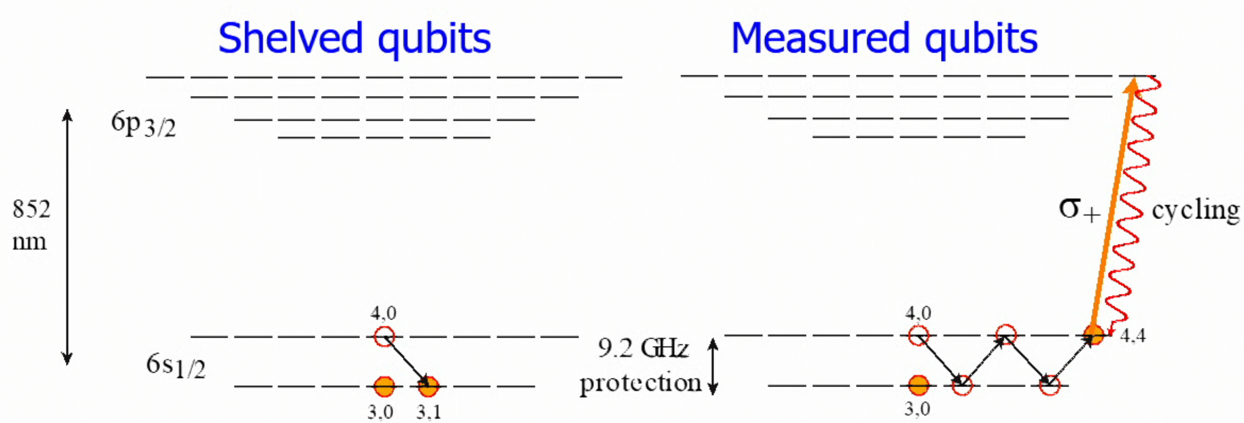

Non-destructive measurements

9-qubit plaquette

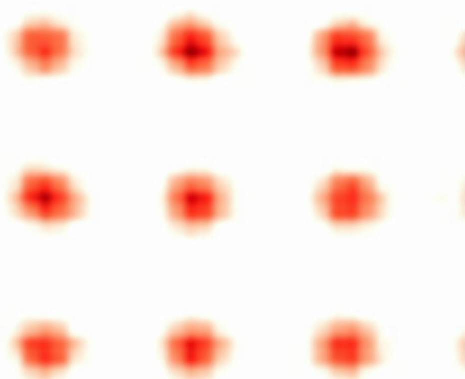

Array averaged retention 0.97

Traps 2.5 mK deep
50% duty cycle chopping
I/I_{sat}=0.3
$\Delta=-2\gamma$
Integration time 4 msec

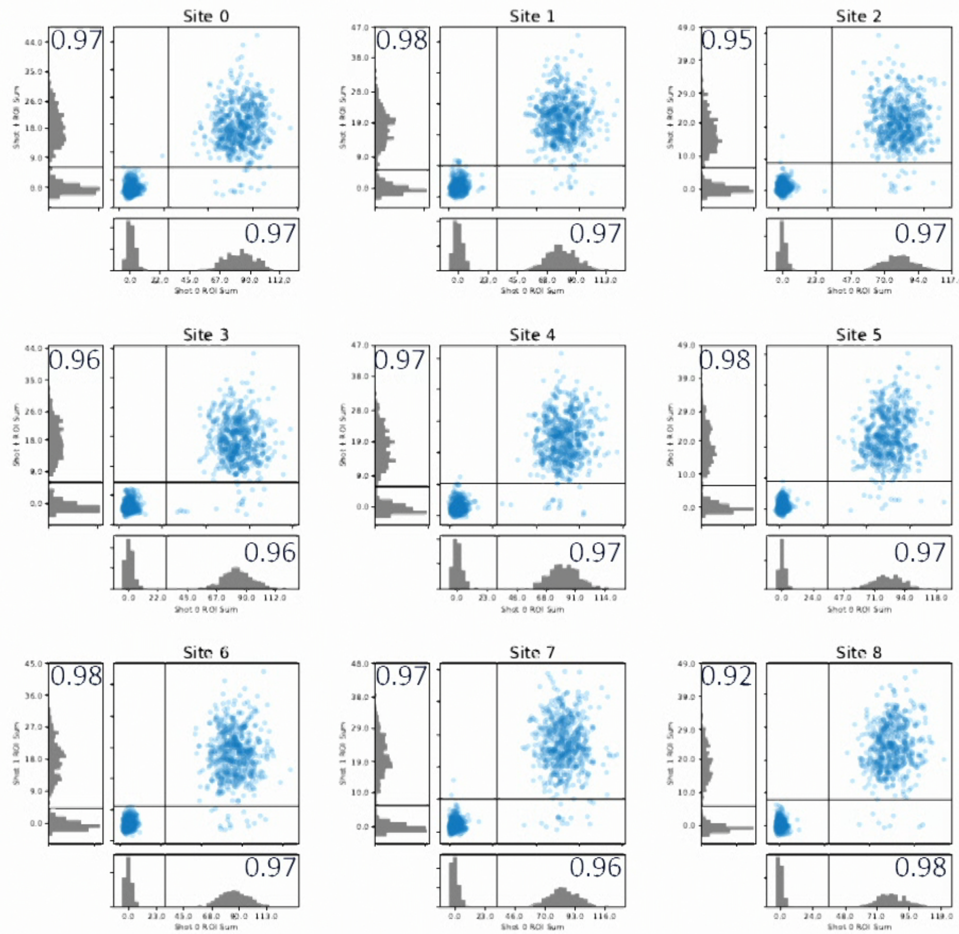

Towards error correction – midcircuit measurements

protect – measure - restore

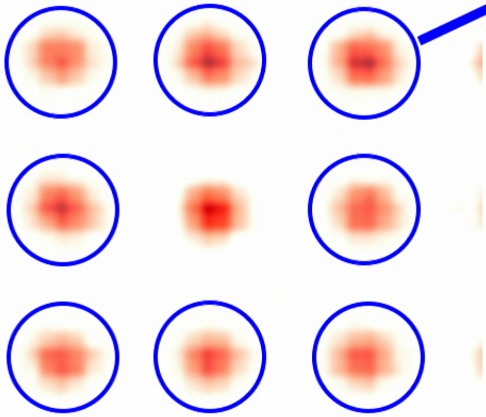

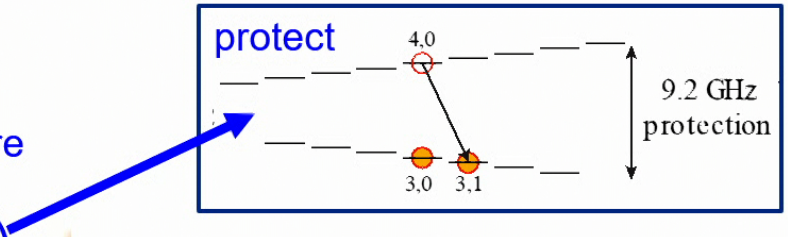

Towards error correction – midcircuit measurements

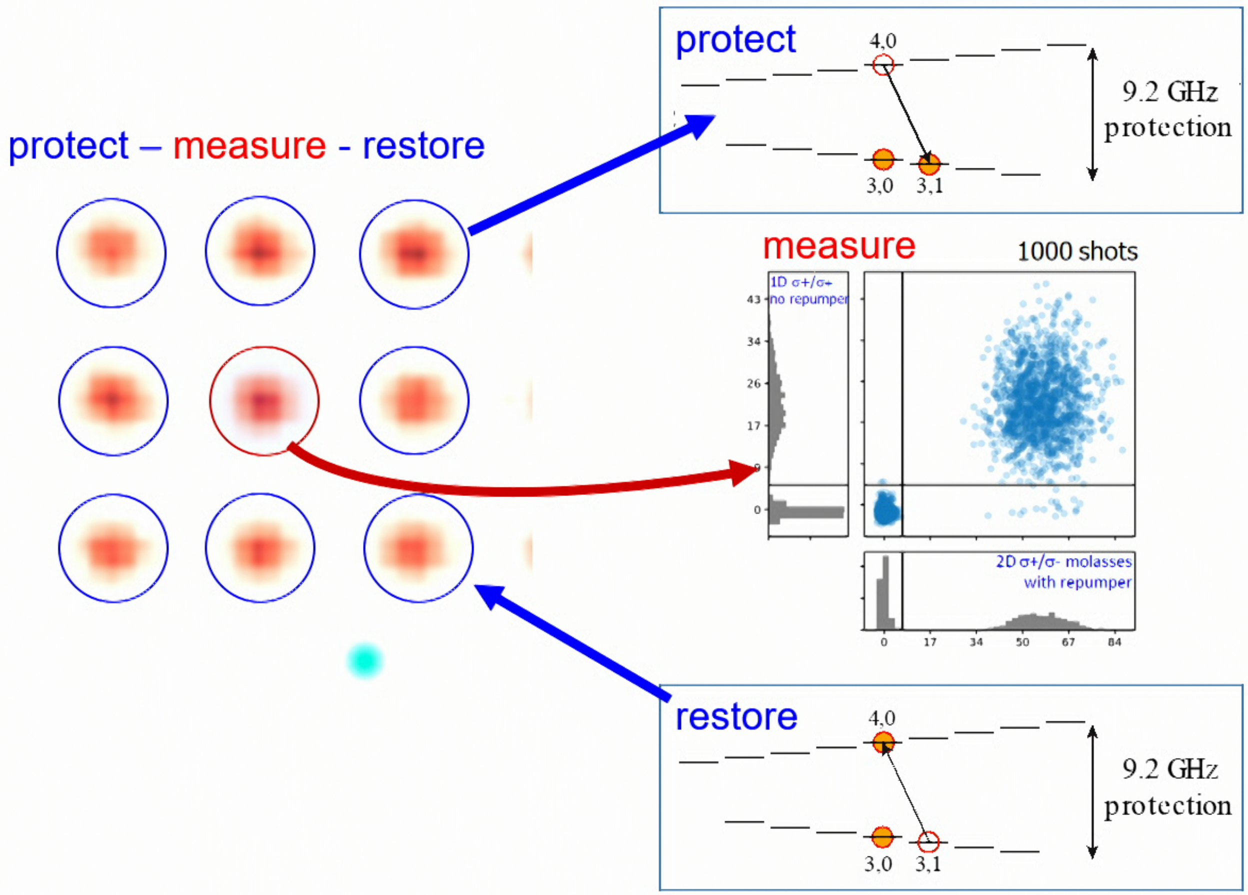

Towards error correction – midcircuit measurements

protect – measure - restore

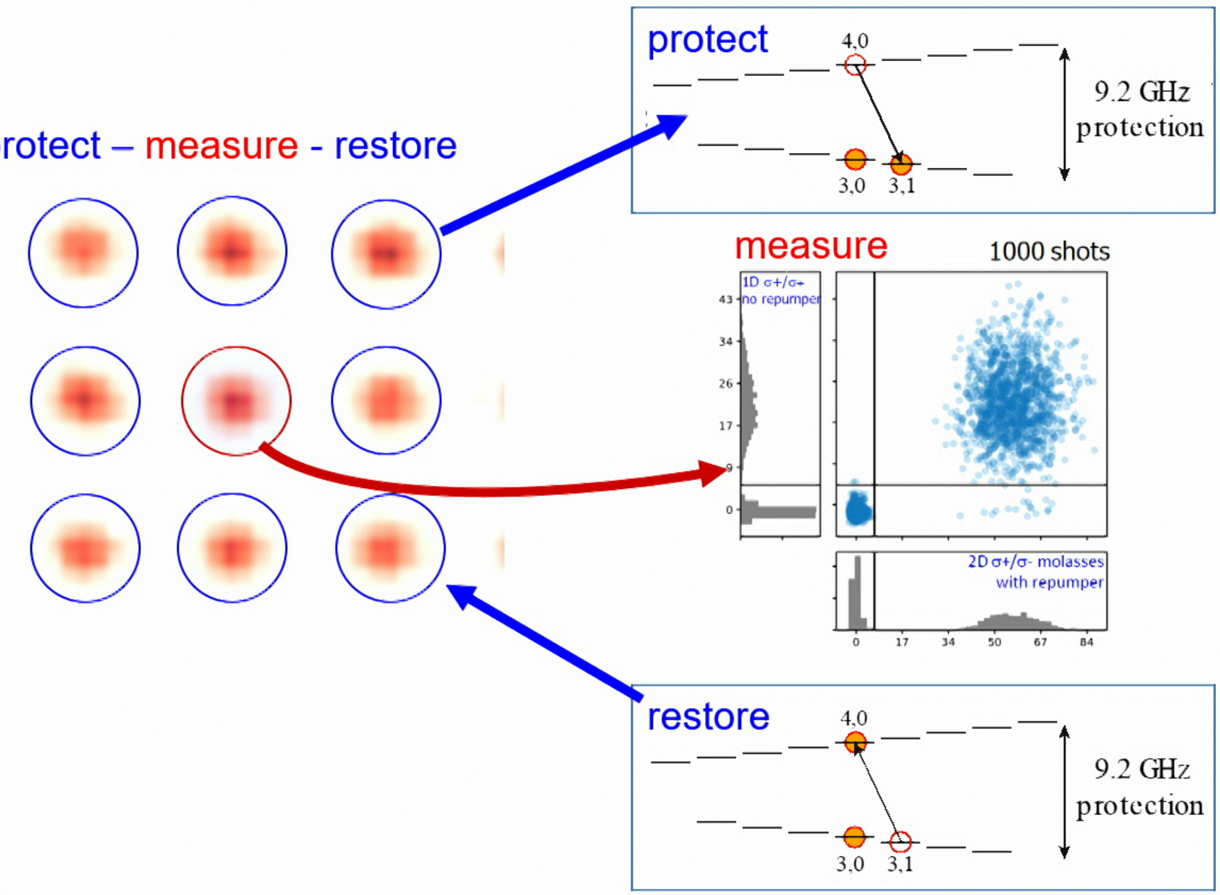

Qubit coherence after restore
F~0.96

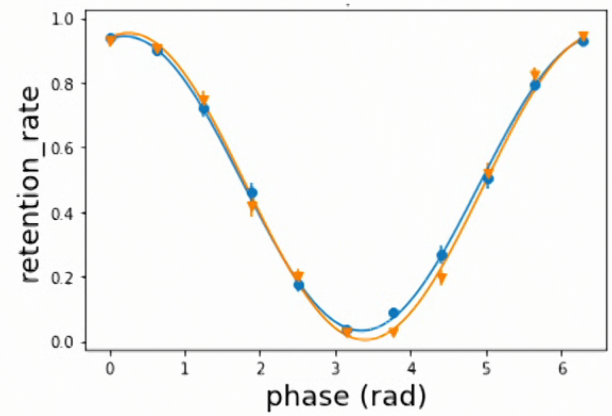

Summary

- Neutral atom qubit arrays provide a scalable platform for quantum computing.
- Gate fidelities: F_{1Q} =0.9998(global), F_{1Q} = 0.993(local), F_{2Q} = 0.965 in 2D array
- Quantum algorithms: GHZ, phase estimation, QAOA
- Towards error correction and logical qubits